Electronic supplementary information for
Photothermal polymerization of benzoxazines

Kevin Reyes-Mateo, Jordi Marquet, Jordi Hernando* and Rosa M. Sebastián*

Table of contents

1. Materials and methods

Materials. Reagents and solvents for the synthesis of **Bz1**-**Bz10** as well as the metal salts employed as polymerization catalysts were purchased and used without further purification. Thin layer chromatography (TLC) was performed using Merck aluminium backed plates of TLC silica gel 60 F254, and flash column chromatography was performed using silica gel (230-400 mesh).

Nuclear magnetic resonance (NMR). ^{1}H NMR spectra were recorded on Bruker DPX250 (250 MHz) and DPX360 (360 MHz) spectrometers in $CDCl_3$, acetone-d_6 and DMSO-d_6. The δ-scale was normalized relative to the residual solvent signal ($CDCl_3$: 7.26 ppm, acetone-d_6: 2.05 ppm and DMSO-d_6: 2.49 ppm).

UV-vis absorption spectrometry. Liquid samples and solutions were measured with an Agilent 8453 UV-visible spectrophotometer using Hellma Analytics glass cuvettes (1-cm and 2-mm light path).

Laser irradiation for photothermal polymerization. Unless indicated otherwise, samples were irradiated with the second harmonic (λ_{exc} = 532 nm, rep rate = 10 Hz, pulse width = 6 ns) of a Nd:YAG pulsed laser (Brilliant, Quantel). The photopolymerization of **Bz3**-$Zn(OTf)_2$ was also attempted with a cw laser at the same wavelength.

Temperature sensing. Temperature monitorization during photoirradiation experiments was conducted using a Testo 735 thermocouple.

Differential scanning calorimetry (DSC). Samples were analyzed with a TA Instruments Q20 calorimeter using Tzero™ pans and lids calibrated with indium (T_m = 429.75 K, ΔH_m = 3267 kJ/mol). For all the samples, we used a heating rate of 10 °C/min and a N_2 flow of 50 mL/min.

Thermal gravimetric analysis (TGA). Samples were recorded with a TA Instruments TGA550 Discovery Series analyzed using a platinum HT crucible. For all the samples, we used a heating rate of 10 °C/min, a heating range of 30 – 800 °C, a N_2 flow of 40 mL/min and an air flow of 60 mL/min.

Dynamic mechanical analysis (DMA). Samples were tested in a TA Instruments DMAQ800 thermo-dynamo-mechanical analysis machine by using the three-point bending mode (F = 1 N/min). DMA experiments were performed on 32 x 12 x 3 mm rectangular polymer pieces prepared by either photothermal or thermal polymerization.

2. Synthesis of Bz1-Bz10

2.1. Synthesis of 1,3,5-triphenyltriazine, 3[1]

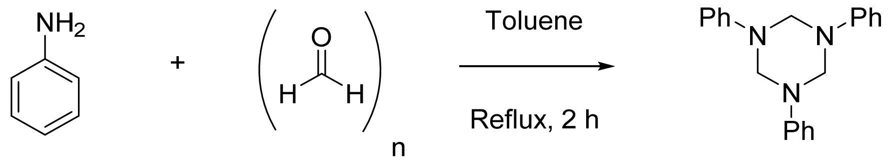

1 **2** **3**

In a round-bottom flask equipped with a Dean-Stark apparatus, previously distilled aniline (**1**, 27.3 mL, 0.3 mol) and paraformaldehyde (**2**, 9.00 g, 0.3 mol) were added in 200 mL of toluene. The mixture was stirred under reflux for 2 h. The reaction crude was cooled down to room temperature, and the white precipitate formed was filtered and washed with *n*-hexane. The solid was dried under reduced pressure and triazine **3** was obtained as a crystalline white solid (19.60 g, 62.2 mmol, 62 %).

Spectroscopic data

^{1}H NMR (360 MHz, $CDCl_3$). δ: 7.21 (t, *J* = 8.0 Hz, 6H), 7.01 (d, *J* = 8.0 Hz, 6H), 6.86 (t, *J* = 7.3 Hz, 3H), 4.89 (s, 6H).

2.2. Synthesis of benzoxazines Bz1-Bz8

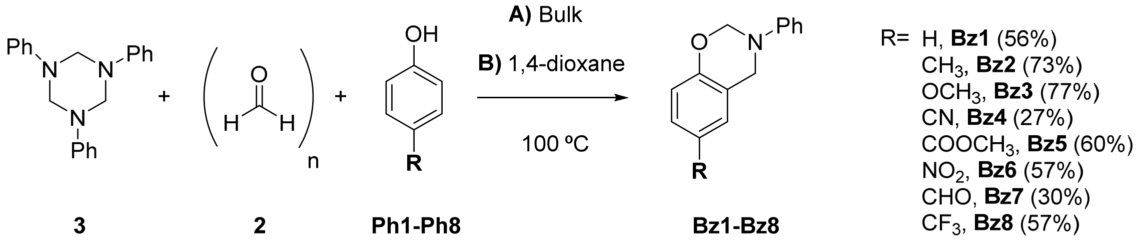

Method A: Bz1,1 **Bz2,**[2] **Bz3,**1 **Bz4,**[3] **Bz5**[4] **and Bz7**[5]

In a round-bottom flask, 1,3,5-triphenyltriazine (**3**, 1 eq.), paraformaldehyde (**2**, 1 eq.) and the respective phenol (**Ph1**-**Ph5** and **Ph7**, 1 eq.) were slowly stirred in bulk and heated up to 100 °C. Once the mixture was melted, stirring was increased during the reaction time (40 min – 2 h). Next, the reaction crude was cooled down to room temperature and dissolved in Et_2O (30 – 50 mL)[a]. The resulted organic phase was washed with 2 M NaOH (3 x 30 – 50 mL) and distilled water (3 x 30 – 50 mL) and finally dried with anhydrous Na_2SO_4. After filtration, the solvent was

---

[a] The addition of Et_2O must be done BEFORE the solution reaches room temperature, since a hard and insoluble solid is formed at this point.

evaporated under vacuum and the obtained benzoxazine was purified by flash column chromatography (silica gel). The exact conditions used for the synthesis and purification of **Bz1-Bz5** and **Bz7** are shown in Table S1.

Table S1. Experimental conditions for the synthesis of benzoxazines **Bz1**-**Bz5** and **Bz7**.

Bz	**Amount of phenol**	$t_{reaction}$	**Flash column chromatography**	**Yield (%)**	**Appearance**
Bz1 (R=H)	2.23 g (23.7 mmol)	2 h	Hexane/DCM (2:1)	56% (2.78 g)	Yellow solid
Bz2 (R=CH_3)	1.30 g (12.0 mmol)	40 min	Hexane/DCM (3:1)	73% (1.97 g)	White solid
Bz3 (R=OCH_3)	3.70 g (29.5 mmol)	2 h	Hexane/DCM (2:1)	77% (5.54 g)	Yellow liquid
Bz4 (R=CN)	1.43 g (12.0 mmol)	1 h	Hexane/DCM (7:3)	27% (0.77 g)	White solid
Bz5 (R=COOEt)	2.10 g (12.4 mmol)	2 h	No purification required	60% (2.10 g)	Yellow solid
Bz7 (R=CHO)	1.46 g (12.0 mmol)	1.5 h	Hexane/DCM (1:2)	30% (0.84 g)	Yellow solid

Spectroscopic data

Bz1: **^{1}H NMR** (360 MHz, $CDCl_3$). δ (ppm): 7.29 (d, *J* = 8.1 Hz, 2H), 7.13 (m, 3H), 7.03 (d, *J* = 7.6 Hz, 1H), 6.95 (t, *J* = 7.0 Hz, 1H), 6.90 (t, *J* = 7.7 Hz, 1H), 6.83 (d, *J* = 8.2 Hz, 1H), 5.38 (s, 2H), 4.65 (s, 2H).

Bz2: **^{1}H NMR** (360 MHz, $CDCl_3$). δ (ppm): 7.25 (m, 2H), 7.10 (d, *J* = 7.6 Hz, 2H), 6.92 (t, *J* = 7.5 Hz, 2H), 6.82 (s, 1H), 6.71 (d, *J* = 8.3 Hz, 1H), 5.34 (s, 2H), 4.60 (s, 2H), 2.25 (s, 3H).

Bz3: **^{1}H NMR** (360 MHz, $CDCl_3$). δ (ppm): 7.29 (m, 2H), 7.12 (d, *J* = 8.0 Hz, 2H), 6.95 (t, *J* = 7.5 Hz, 1H), 6.77 (d, *J* = 8.8 Hz, 1H), 6.71 (dd, *J* = 8.8 Hz, *J* = 2.8 Hz, 1H), 6.58 (d, *J* = 2.8 Hz, 1H), 5.33 (s, 2H), 4.62 (s, 2H), 3.75 (s, 3H).

Bz4: **^{1}H NMR** (360 MHz, $CDCl_3$). δ (ppm): 7.41 (dd, *J* = 8.5 Hz, *J* = 2.1 Hz, 1H), 7.30 (m, 3H), 7.10 (d, *J* = 8.1 Hz, 2H), 7.00 (t, *J* = 7.4 Hz, 1H), 6.87 (d, *J* = 8.5 Hz, 1H), 5.45 (s, 2H), 4.66 (s, 2H).

Bz5: **^{1}H NMR** (250 MHz, $CDCl_3$). δ (ppm): 7.81 (dd, *J* = 8.7 Hz, *J* = 1.7 Hz, 1H), 7.76 (d, *J* = 2.1 Hz, 1H), 7.27 (t, *J* = 7.7 Hz, 2H), 7.10 (d, *J* = 7.6 Hz, 2H), 6.95 (t, *J* = 7.6 Hz, 1H), 6.82 (d, *J* = 8.7 Hz, 1H), 5.42 (s, 2H), 4.66 (s, 2H), 4.34 (q, *J* = 7.0 Hz, 2H), 1.37 (t, *J* = 6.8 Hz, 3H).

Bz7: **^{1}H NMR** (250 MHz, $CDCl_3$). δ (ppm): 9.83 (s, 1H), 7.65 (d, *J* = 7.6 Hz, 1H), 7.59 (s, *J* = , 2H), 7.29 (d, *J* = 7.6 Hz, 1H), 7.11 (d, *J* = 8.2 Hz, 2H), 6.97 (t, *J* = 7.0 Hz, 1H), 6.91 (d, *J* = 8.8 Hz, 1H), 5.46 (s, 2H), 4.70 (s, 2H).

Method B: Bz61 **and Bz8**4

In a round-bottom flask, 1,3,5-triphenyltriazine (**3**), paraformaldehyde (**2**, 1 eq.) and the respective phenol (**Ph6** and **Ph8**, 1 eq.) were mixed in 1,4-dioxane (15 mL). The solution was stirred for a given time at 100 °C. The reaction crude was cooled down to room temperature and the solvent was evaporated under vacuum. A yellow liquid was obtained and, after rinsing with Et_2O, the desired benzoxazine was achieved that was purified by flash column chromatography (silica gel). The exact conditions used for the synthesis and purification of **Bz6** and **Bz8** are shown in Table S2.

Table S2. Experimental conditions for the synthesis of benzoxazines **Bz6** and **Bz8**.

Bz	**Amount of phenol**	***t***	**Flash column chromatography**	**Yield (%)**	**Appearance**
Bz6 (R=NO_2)	1.58 g (5.0 mmol)	18 h	Hexane/DCM (1:1)	57% (2.20 g)	Yellow solid
Bz8 (R=CF_3)	2.3 g (8.2 mmol)	2 h	Hexane/DCM (1:1)	57% (1.31 g)	White solid

<u>**Spectroscopic data**</u>

Bz6: **^{1}H NMR** (250 MHz, $CDCl_3$). δ (ppm): 8.06-7.96 (m, 2H), 7.28 (t, *J* = 8.1 Hz, 2H), 7.10 (d, *J* = 7.5 Hz, 2H), 6.99 (t, *J* = 7.3 Hz, 1H), 6.87 (d, *J* = 8.1 Hz, 1H), 5.47 (s, 2H), 4.70 (s, 2H).

Bz8: **^{1}H NMR** (300 MHz, $CDCl_3$). δ (ppm): 7.51 (s, 1H), 7.44 (d, *J* = 8.2 Hz, 1H), 7.28 (d, *J* = 7.8 Hz, 1H), 7.24 (t, *J* = 7.7 Hz, 1H), 7.20 (d, *J* = 8.0 Hz, 2H), 7.18 (t, *J* = 7.6 Hz, 1H), 6.93 (m, 1H), 5.57 (s, 2H), 4.83 (s, 2H).

2.3. Synthesis of bisbenzoxazine **Bz9**2

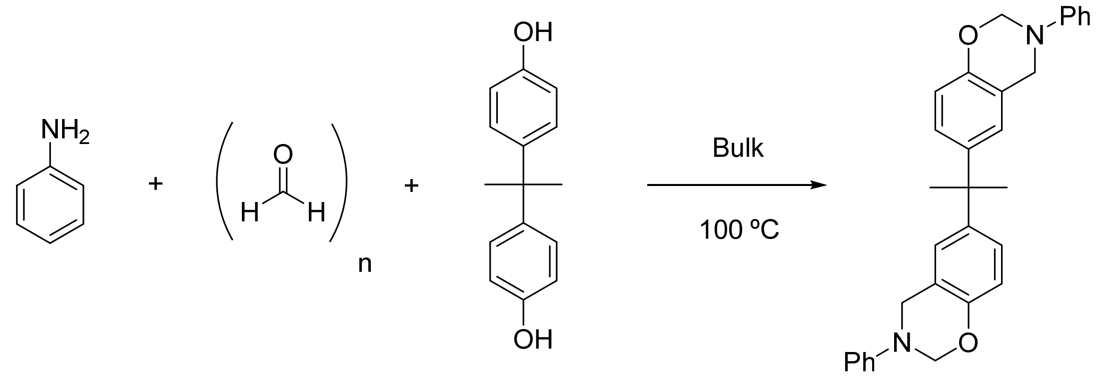

1 **2** **Ph9** **Bz9**

In a round-bottom flask, aniline (**1**, 1.8 mL, 20.0 mmol), paraformaldehyde (**2**, 1.20 g, 40.0 mmol) and bisphenol A (**4**, 2.30 g, 10.0 mmol) were mixed without solvent. The resulting solution was stirred for 45 min at 100 °C. The reaction crude was cooled down to room temperature and dissolved in Et_2O (≈ 40 mL).[b] The resulting solution was dried in anhydrous Na_2SO_4 and filtered. The solvent was evaporated under vacuum and a yellowish solid foam was obtained.[c] The resulting product was purified by flash column chromatography (silica gel, hexane/AcOEt (9:1)). Bisbenzoxazine **Bz9** was afforded in this way as a yellowish solid foam (2.50 g, 5.4 mmol, 54 %).

<u>Spectroscopic data</u>

^{1}H NMR (360 MHz, $(CD_3)_2CO$). δ (ppm): 7.23 (t, *J* = 8.0 Hz, 4H), 7.14 (dd, *J* = 9.0 Hz, *J* = 1.2 Hz, 4H), 7.00 (d, *J* = 2.2 Hz, 2H), 6.92 (dd, *J* = 8.7 Hz, *J* = 2.5 Hz, 2H), 6.86 (t, *J* = 7.2 Hz, 2H), 6.62 (d, *J* = 8.7 Hz, 2H), 5.40 (s, 4H), 4.63 (s, 4H), 1.56 (s, 6H).

2.4. Synthesis of benzoxazine **Bz10**1

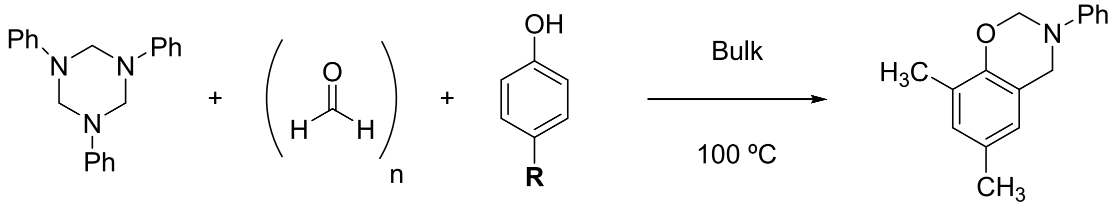

3 **2** **Ph10** **Bz10**

---

[b] The addition of Et_2O must be done BEFORE the solution reaches to room temperature, since a hard and insoluble solid is formed at this point.

[c] A 500 mL round-bottom flask is recommended to be used for these reagent quantities. When the solvent is evaporated under vacuum, a foam is formed that quickly expands. This is why a high volume is required as it is drying.

A mixture of phenol **Ph10** (1.83 g, 15 mmol), paraformaldehyde **2** (450 mg, 15 mmol), and 1,3,5-triphenylhexahydro-1,3,5-triazine **3** (1.575 g, 5 mmol) was stirred in air at 100 ℃ for 2 h. After cooled to room temperature, the mixture was dissolved in Et_2O and washed three times with 2 M NaOH and three times with water. The organic phase was dried with anhydrous Na_2SO_4, the diethyl ether was removed at low pressure and **Bz10** was obtained as a yellow oil without further purification (2.40 g, 10.1 mmol, 67%).

Spectroscopic data

^{1}H NMR (250 MHz, $CDCl_3$) δ (ppm): 7.25-7.31 (m, 2H, Ar-H, overlapping with the signal of $CHCl_3$), 7.12 (d, *J* = 7.5 Hz, 2H, Ar-H), 6.93 (t, *J* = 7.0 Hz, 1H, Ar-H), 6.81 (s, 1H, Ar-H), 6.69 (s, 1H, Ar-H), 5.37 (s, 2H, O-CH_2-N), 4.59 (s, 2H, Ar-CH_2-N), 2.23 (s, 3H, CH_3), 2.16 (s, 3H, CH_3).

3. Spectrophotometric characterization of Bz-catalyst systems

3.1. UV-vis absorption spectra of Bz-catalyst systems

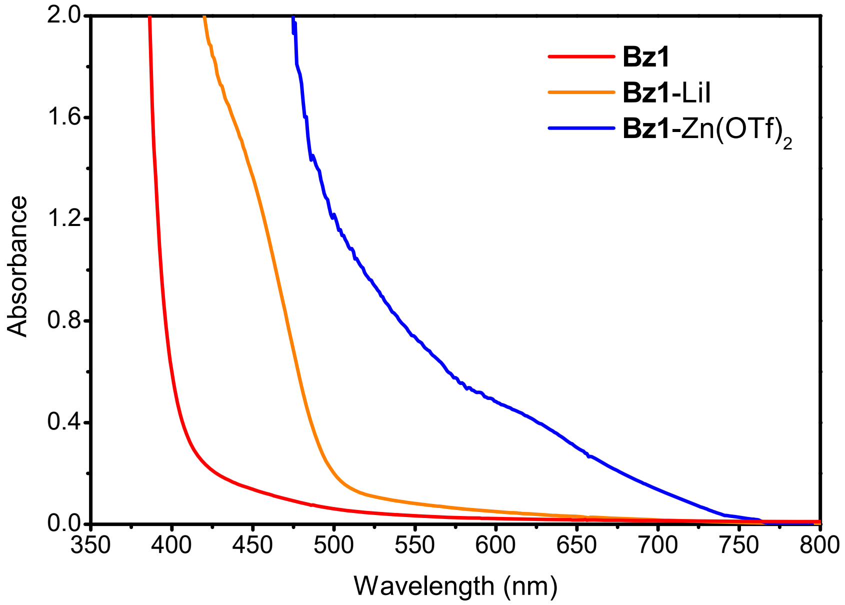

Fig. S1 UV-vis absorption spectra of **Bz1**, **Bz1**-LiI (c_{LiI} = 50 mol % relative to monomer content) and **Bz1**-Zn(OTf)$_2$ ($c_{\mathrm{Zn(OTf)2}}$ = 15 mol % relative to monomer content) in acetone ($c_{\mathbf{Bz1}}$ = 3.9 M). A 2 mm-thick glass cuvette was used.

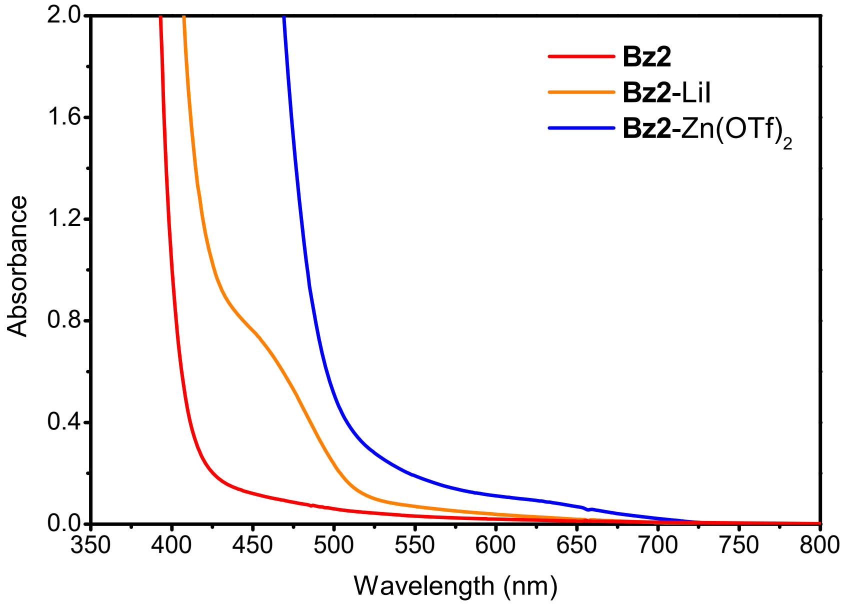

Fig. S2 UV-vis absorption spectra of **Bz2**, **Bz2**-LiI (c_{LiI} = 50 mol % relative to monomer content) and **Bz2**-Zn(OTf)$_2$ ($c_{\mathrm{Zn(OTf)2}}$ = 15 mol % relative to monomer content) in acetone ($c_{\mathbf{Bz2}}$ = 3.9 M). A 2 mm-thick glass cuvette was used.

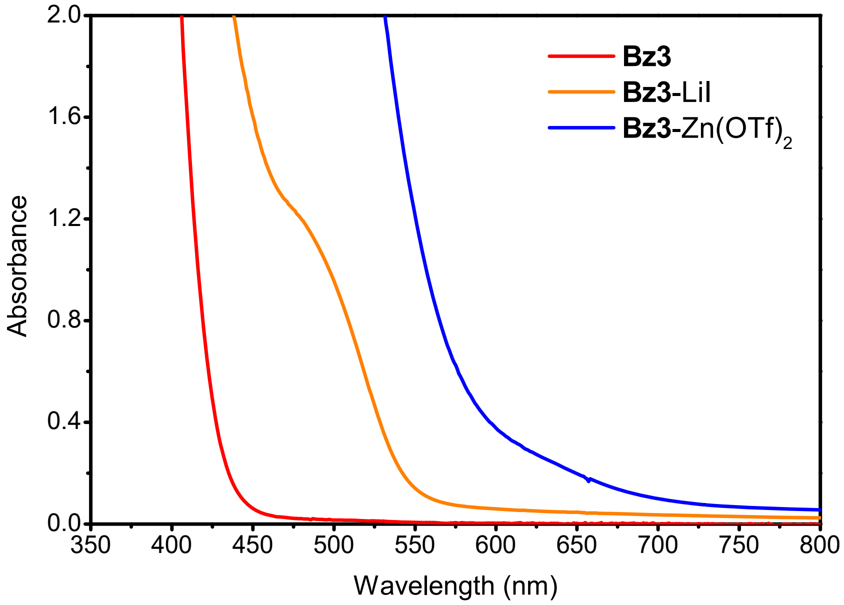

Fig. S3 UV-vis absorption spectra of **Bz3**, **Bz3**-LiI (c_{LiI} = 50 mol % relative to monomer content) and **Bz3**-Zn(OTf)$_2$ ($c_{\mathrm{Zn(OTf)2}}$ = 15 mol % relative to monomer content) in bulk liquid. A 2 mm-thick glass cuvette was used.

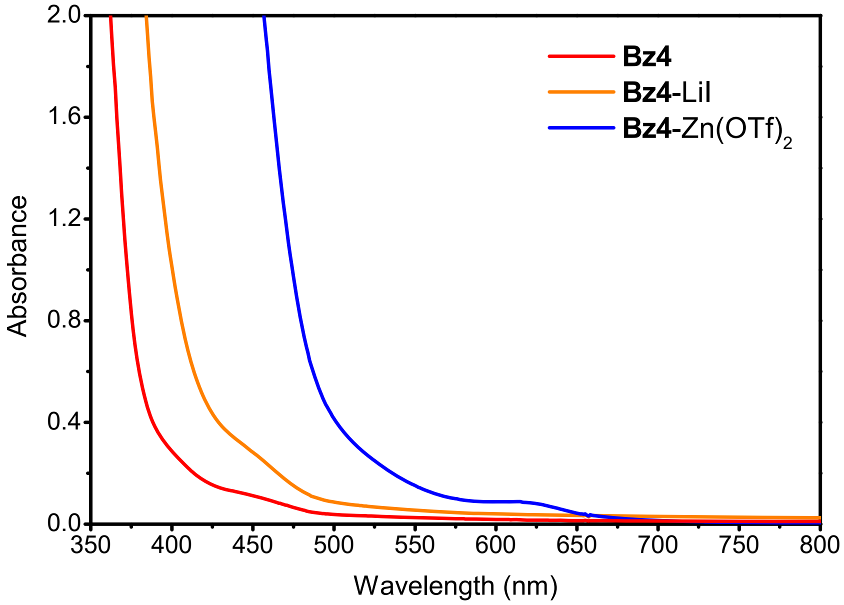

Fig. S4 UV-vis absorption spectra of **Bz4**, **Bz4**-LiI (c_{LiI} = 50 mol % relative to monomer content) and **Bz4**-Zn(OTf)$_2$ ($c_{\mathrm{Zn(OTf)2}}$ = 15 mol % relative to monomer content) in acetone ($c_{\mathbf{Bz4}}$ = 1.2 M). A 2 mm-thick glass cuvette was used.

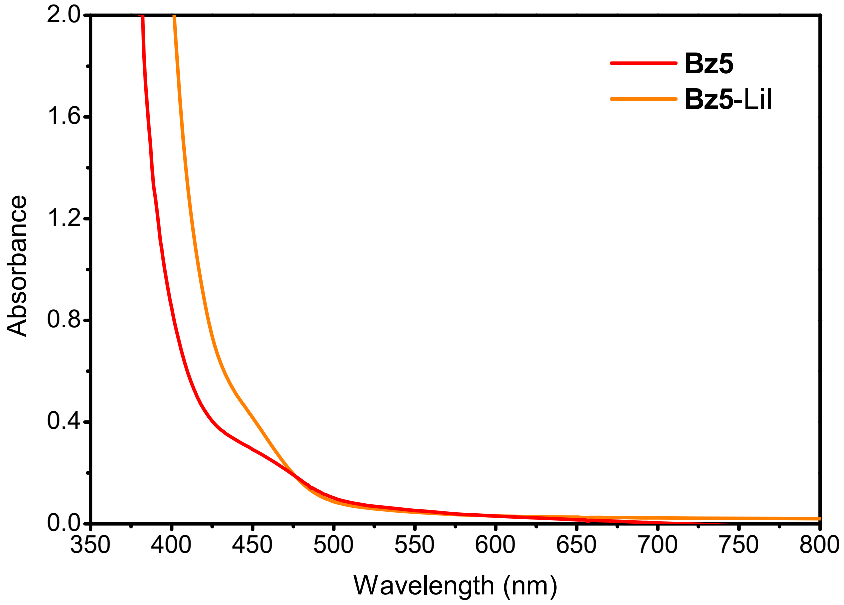

Fig. S5 UV-vis absorption spectra of **Bz5** and **Bz5**-LiI (c_{LiI} = 50 mol % relative to monomer content) in acetone ($c_{\mathbf{Bz5}}$ = 2.4 M). A 2 mm-thick glass cuvette was used.

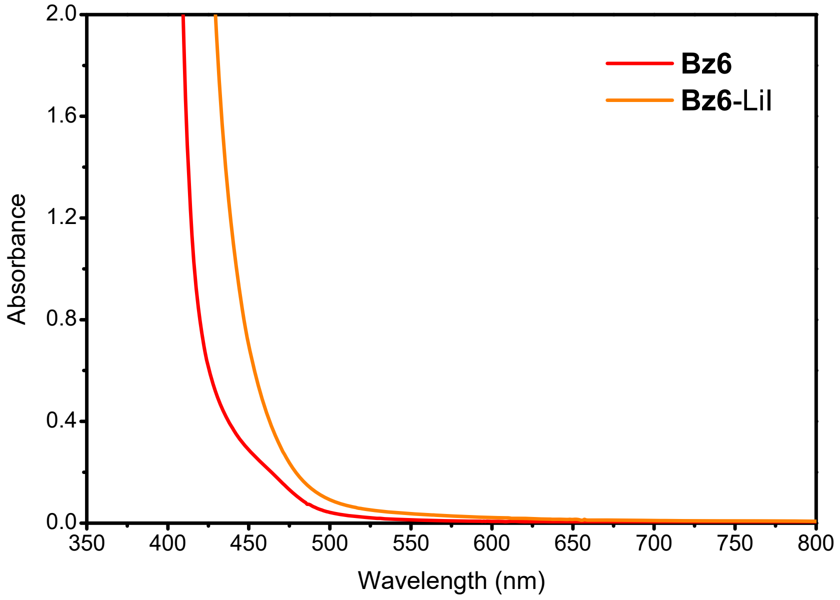

Fig. S6 UV-vis absorption spectra of **Bz6** and **Bz6**-LiI (c_{LiI} = 50 mol % relative to monomer content) in acetone ($c_{\mathbf{Bz6}}$ = 1.0 M). A 2 mm-thick glass cuvette was used.

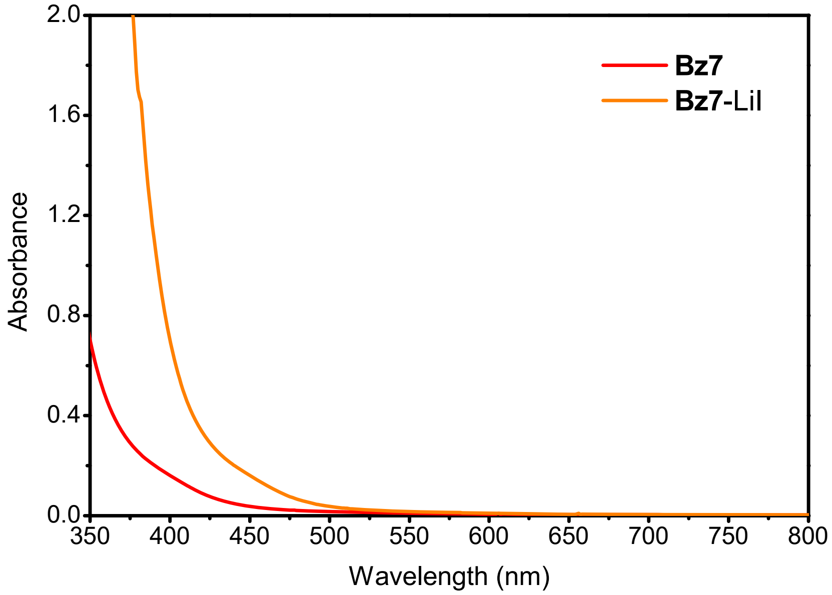

Fig. S7 UV-vis absorption spectra of **Bz7** and **Bz7**-LiI (c_{LiI} = 50 mol % relative to monomer content) in acetone ($c_{\mathbf{Bz7}}$ = 2.0 M). A 2 mm-thick glass cuvette was used.

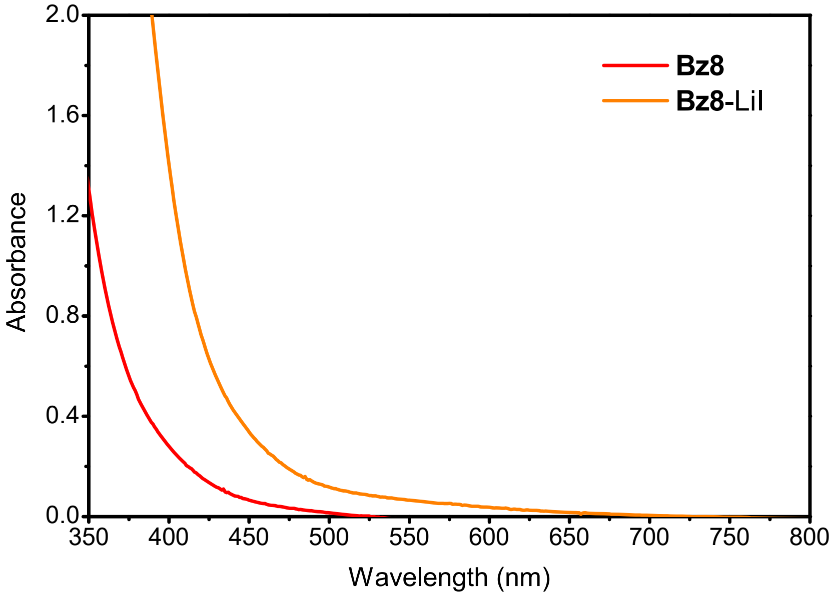

Fig. S8 UV-vis absorption spectra of **Bz8** and **Bz8**-LiI (c_{LiI} = 50 mol % relative to monomer content) in acetone ($c_{\mathbf{Bz8}}$ = 1.9 M). A 2 mm-thick glass cuvette was used.

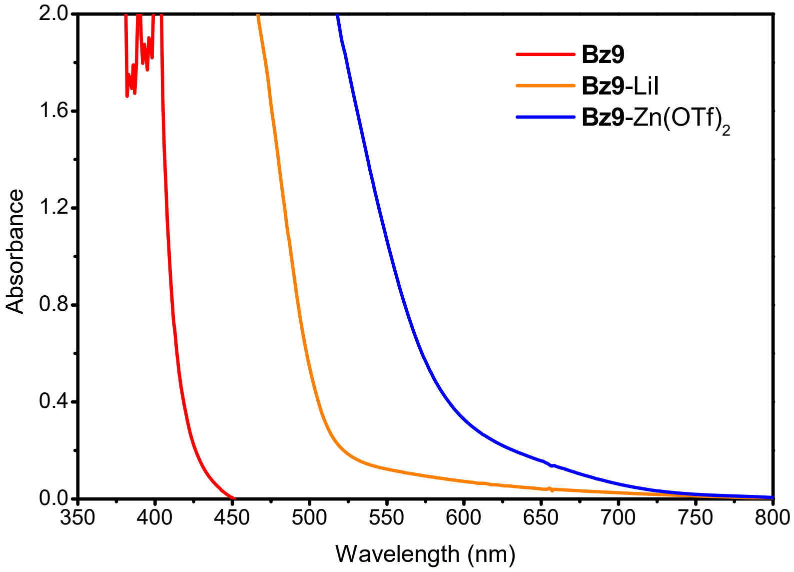

Fig. S9 UV-vis absorption spectra of **Bz9**, **Bz9**-LiI (c_{LiI} = 50 mol % relative to monomer content) and **Bz9**-Zn(OTf)$_2$ ($c_{Zn(OTf)2}$ = 15 mol % relative to monomer content) in acetone ($c_{\mathbf{Bz9}}$ = 2.4 M). A 2 mm-thick glass cuvette was used.

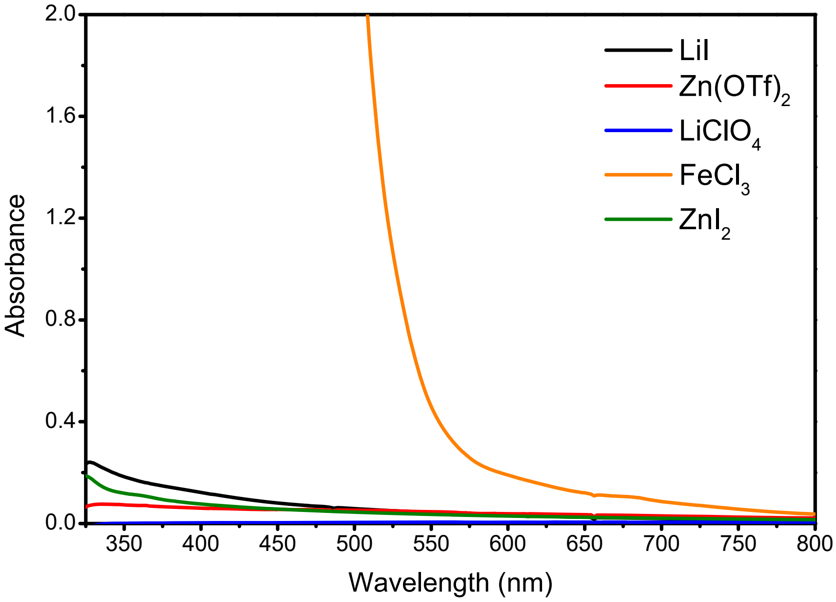

Fig. S10 UV-vis absorption spectra of LiI (c_{LiI} = 1 M), Zn(OTf)$_2$ ($c_{Zn(OTf)2}$ = 0.3 M), LiClO$_4$ (c_{LiClO4} = 0.3 M), FeCl$_3$ (c_{FeCl3} = 0.3 M) and ZnI$_2$ (c_{ZnI2} = 0.3 M) in acetone.

3.2. Studies of metal ion coordination with Bz3 and PBz3

To determine the stoichiometries and association constants for the complexation between metal ions and benzoxazine monomers and polymers, we followed the same procedure previously used by us for similar systems.[6] In particular, we used UV-vis spectrophotometry to monitor the spectral changes induced when: (a) adding increasing concentrations of LiI to neat liquid **Bz3** (Fig. S11a); (b) adding increasing concentrations of LiI to an acetone solution of a polybenzoxazine obtained by thermal polymerization of **Bz3** (Fig. S11b). The differences in absorbance measured in the visible region upon metal salt addition were then plotted against the metal salt concentration (λ_{abs} = 480 and 500 nm for Fig. S11a and S11b, respectively) and fitted to the Benesi–Hildebrand equation (1). In this equation, A is the absorbance upon metal salt addition, A_0 is the absorbance without metal salt, ε_c is the molar absorption coefficient of the complex, ε_0 is the molar absorption coefficient of the initial compound, $[N_0]$ is the concentration of the initial compound, K_a is the association constant, [M] is the concentration of the metal salt for each addition, and n is the stoichiometric ratio.

$$\frac{1}{A-A_0}=\frac{1}{(\varepsilon_c-\varepsilon_0)[N_0]}+\frac{1}{(\varepsilon_c-\varepsilon_0)[N_0]K_a}\frac{1}{[M]^n} \qquad (1)$$

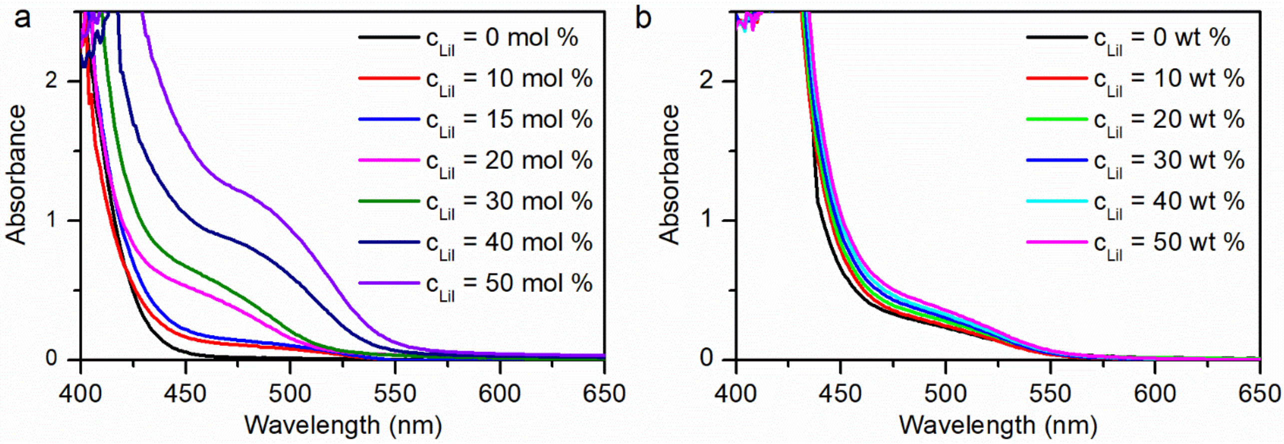

Fig. S11 (a) Variation of the UV-vis absorption spectrum of neat **Bz3** upon addition of increasing concentrations of LiI relative to monomer content. (b) Variation of the UV-vis absorption of thermally polymerized **PBz3** in acetone (c_{PBz3} = 20 mg mL^{-1}) upon addition of increasing concentrations of LiI relative to polymer content.

4. Polymerization of Bz and Bz-catalyst systems

4.1. Preparation of Bz-catalyst systems for thermal and photothermal polymerization

Each given (bis)benzoxazine (0.2 – 0.3 g for **Bz1**, **Bz2** and **Bz4**-**Bz9**, 0.5 mL for **Bz3** and **Bz10**) was mixed with the catalyst of interest (typically, 15 mol % relative to monomer content) in a few milliliters of acetone.[d] Once the mixture was completely solved, acetone was removed under reduced pressure and the corresponding benzoxazine-catalyst system was afforded.

4.2. Determination of monomer conversion

The conversion of all tested benzoxazine monomers during polymerization reactions was determined by ^{1}H NMR using previously reported equation 2.[7,8] In this equation: (a) X is the integration of the ^{1}H NMR signals characteristic of the methylene units in the oxazine ring of the unreacted monomers (δ = 4.6 and 5.4 ppm in $CDCl_3$); (b) Y is the sum of the integrals of the methylene signals of the unreacted monomers and the formed polymers (δ = 3.5 – 6.0 ppm in $CDCl_3$) at a given polymerization time.

$$Conversion\ (\%) = \left[{}^{(Y-2X)}\!/_{Y}\right] \cdot 100 \qquad (2)$$

4.3. Thermal polymerization

Neat benzoxazine thermal polymerization: Each of the (bis)benzoxazines of interest was heated in a sand bath at 180 °C for 2 h.

Thermal polymerization of benzoxazine-catalyst systems: Each of the (bis)benzoxazine-catalyst samples prepared (see section 4.1) was heated in a sand bath at 180 °C for 2 h.

Determination of thermal polymerization temperature (T_P): DSC was used to determine the thermal polymerization temperature of neat Bz monomers and monomer-catalyst systems. Two main thermal transitions were identified in the thermograms of these samples: (a) an endothermic signal arising from the melting of the Bz monomer (except for liquid **Bz3**); (b) an exothermic peak assigned to the polymerization reaction. The onset and peak temperatures of the DSC polymerization signal determined for all the samples under study are given in Table S3, while the corresponding thermograms are shown in Figs. S12-S21.

---

[d] Huge solvent volumes are not required for LiI, since its solubility in acetone is around 400 mg/mL. By contrast, $Zn(OTf)_2$ is barely soluble in acetone at room temperature. For this reason, the metal salt must be solved in hot acetone under vigorous stirring.

Table S3. Thermal polymerization temperature of neat Bz monomers and Bz-catalyst systems.

Bz	Catalyst	c_{catalyst} (mol %)[a]	$T_{p,\ onset}$ (°C)	$T_{p,\ peak}$ (°C)
Bz1	-	-	265.1	269.7
	LiI	15	184.7	194.0
	$Zn(OTf)_2$	15	61.8	77.2
Bz2	-	-	263.9	273.6
	LiI	15	189.6	201.2
	$Zn(OTf)_2$	15	77.2	87.0
Bz3	-	-	249.4	258.9
	LiI	15	141.2	159.4
	$Zn(OTf)_2$	15	56.4	82.4
Bz4	-	-	220.9	225.0
	LiI	15	167.5	180.4
	$Zn(OTf)_2$	15	93.5	99.6
Bz5	-	-	243.9	249.0
	LiI	15	171.1	188.9
Bz6	-	-	189.4	194.5
	LiI	15	153.9	167.2
Bz7	-	-	223.9	229.2
	LiI	15	138.1	159.5
Bz8	-	-	248.5	250.6
	LiI	15	181.2	190.6
Bz9	-	-	214.6	232.3
	LiI	15	160.2	182.8
Bz10	-	-	271.2	281.9
	LiI	15	177.8	199.5

[a] Relative to monomer concentration.

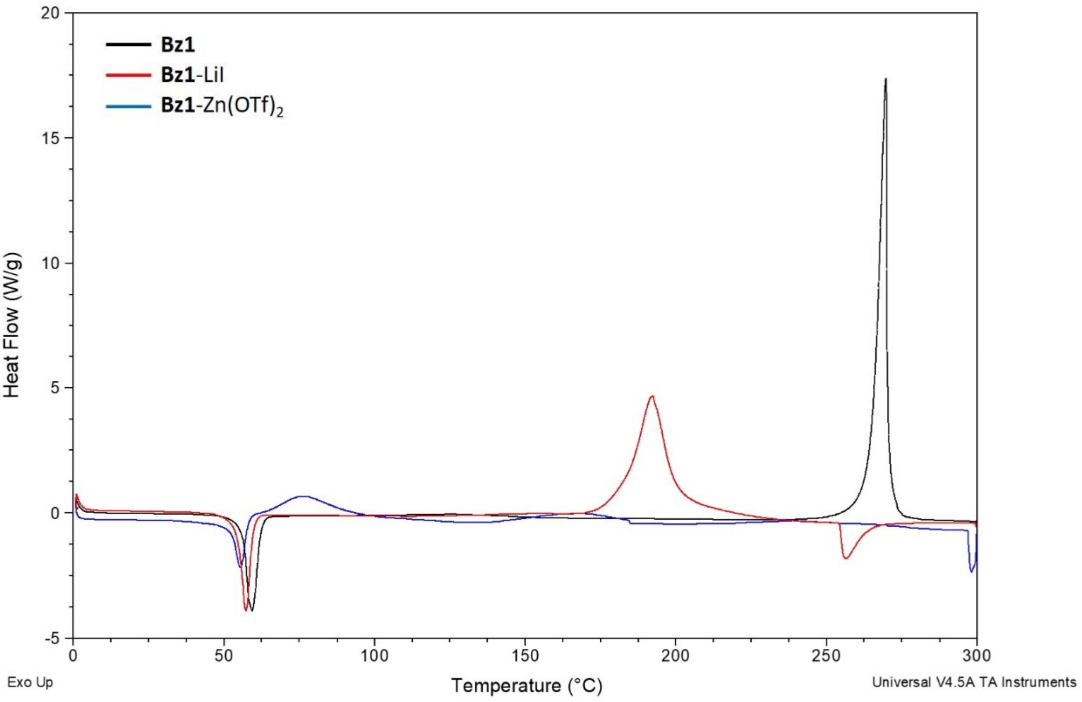

Fig. S12 DSC thermogram of neat **Bz1** and **Bz1**-catalyst systems.

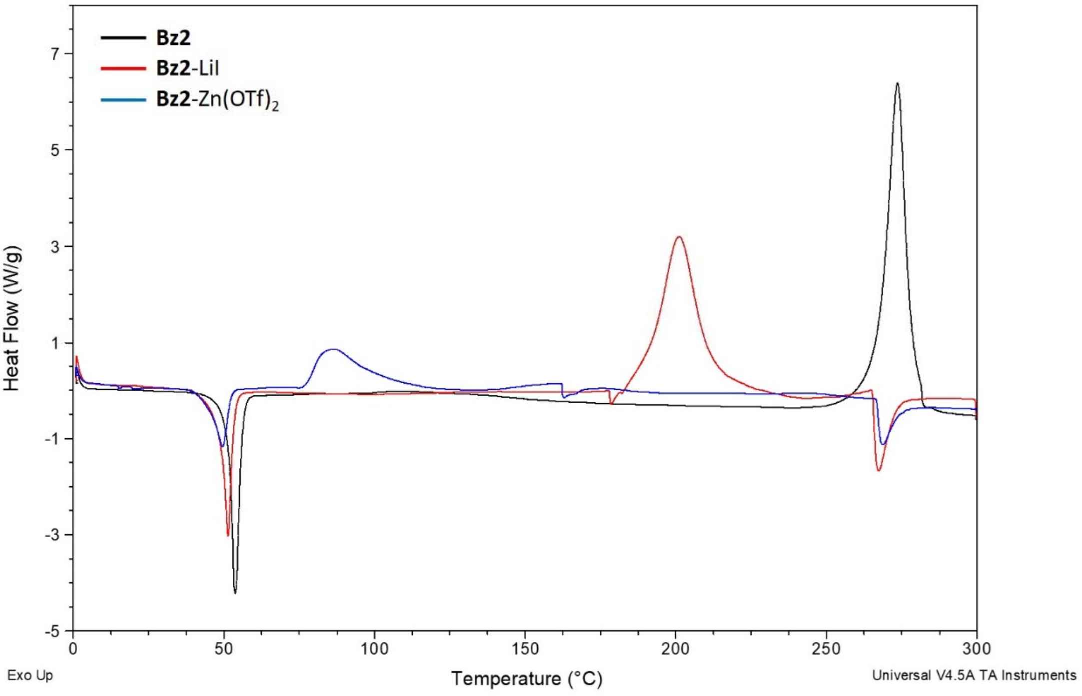

Fig. S13 DSC thermogram of neat **Bz2** and **Bz2**-catalyst systems.

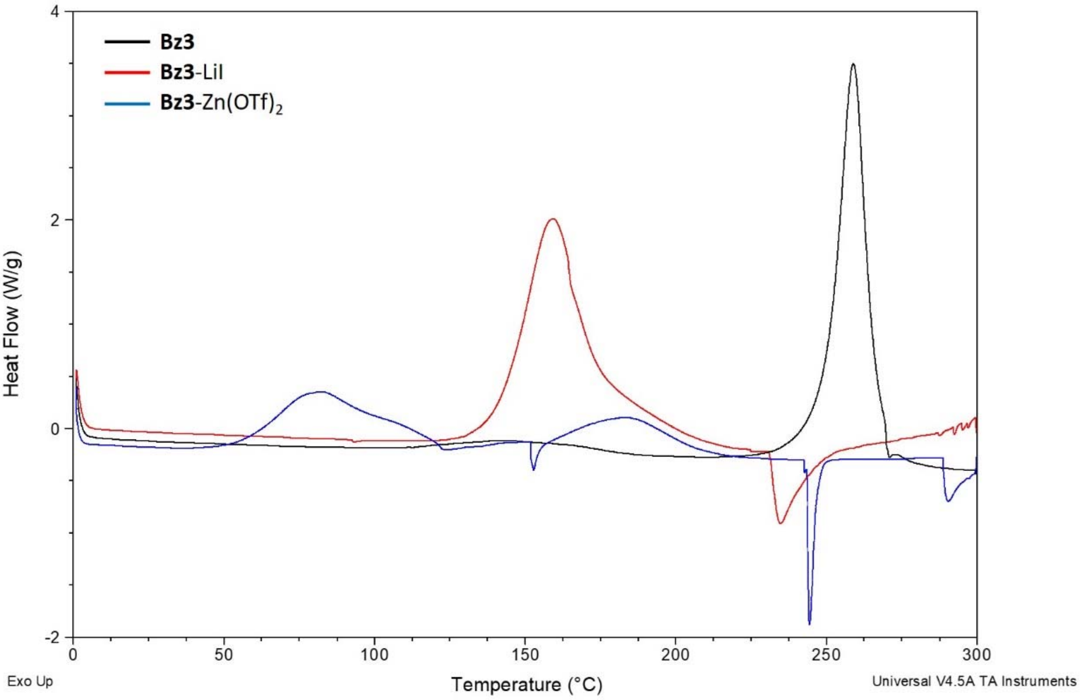

Fig. S14 DSC thermogram of neat **Bz3** and **Bz3**-catalyst systems.

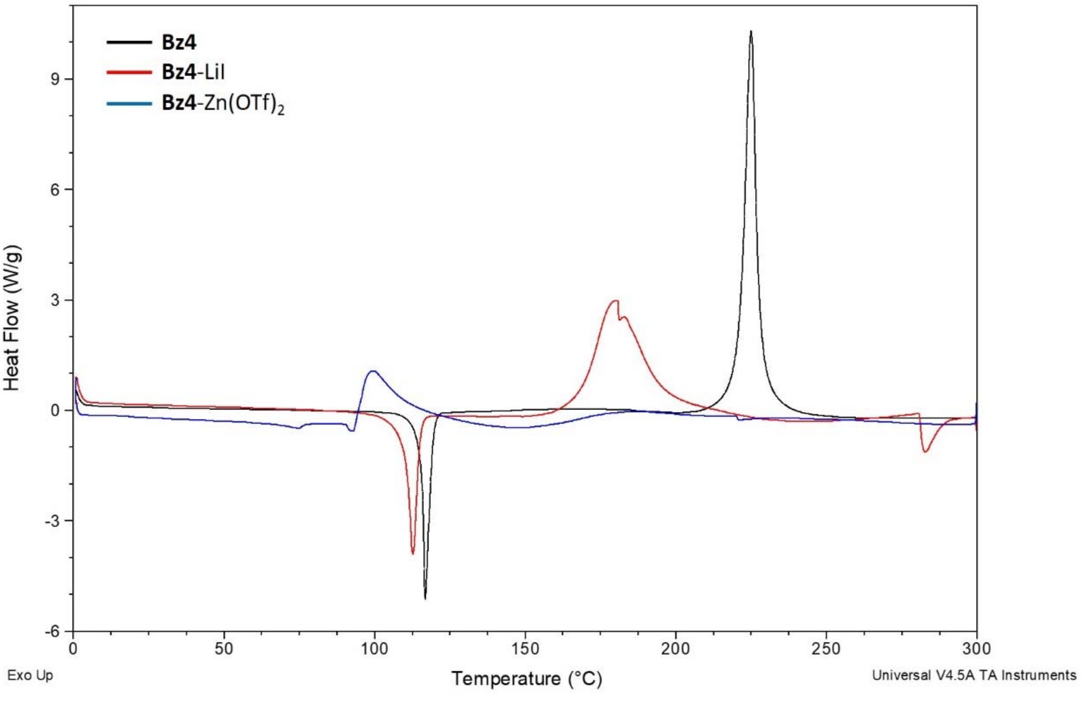

Fig. S15 DSC thermogram of neat **Bz4** and **Bz4**-catalyst systems.

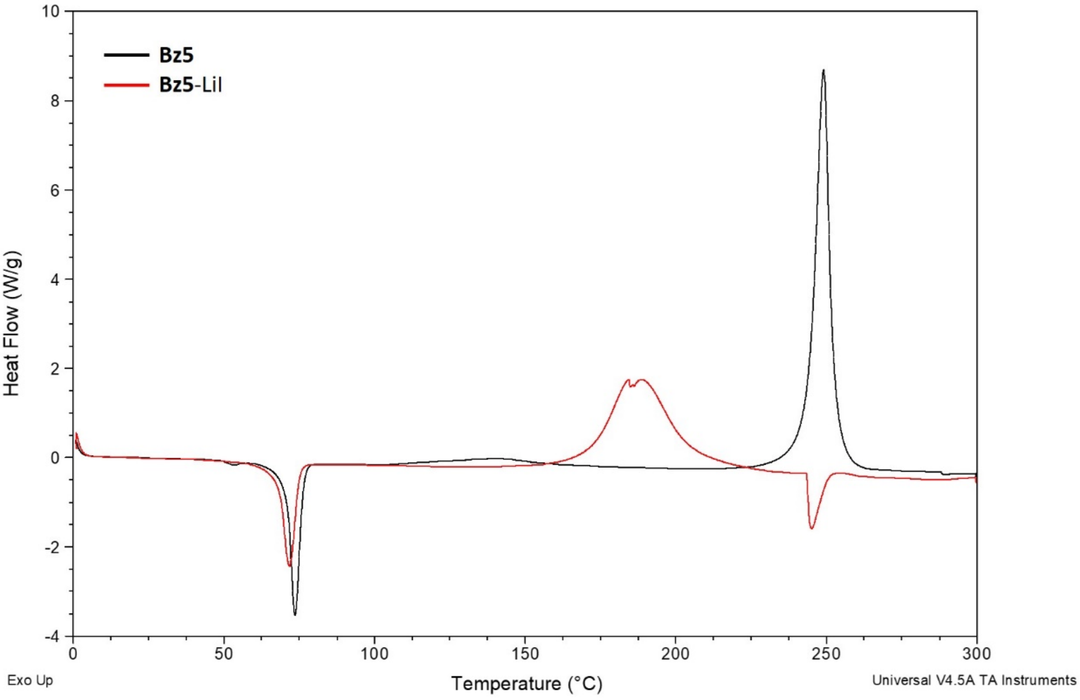

Fig. S16 DSC thermogram of neat **Bz5** and **Bz5**-catalyst systems.

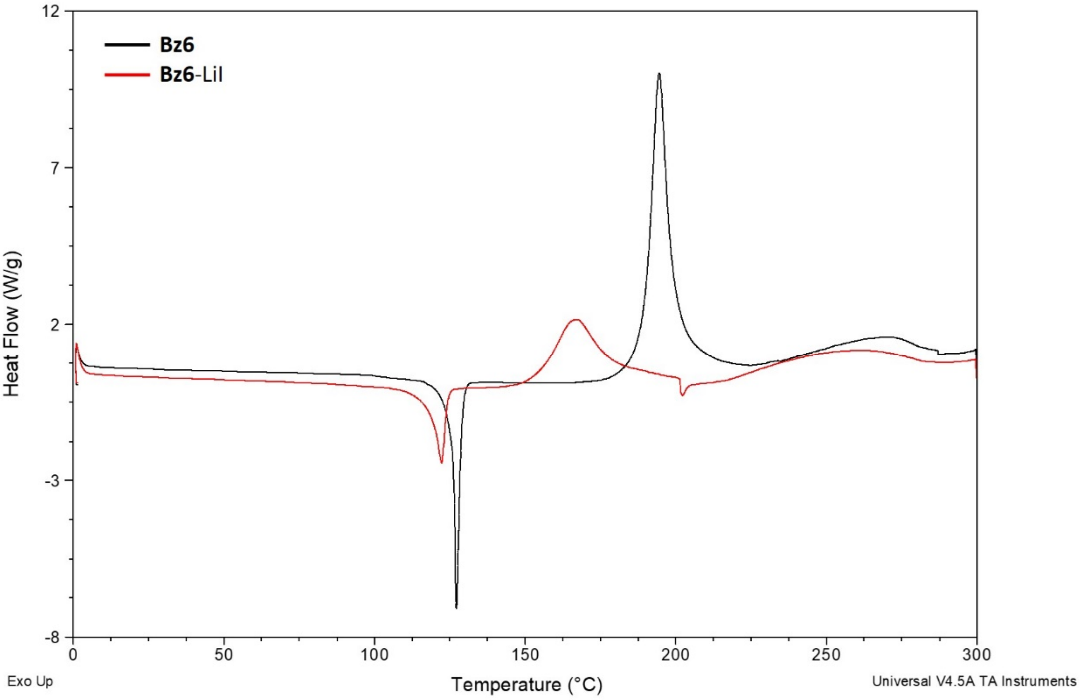

Fig. S17 DSC thermogram of neat **Bz6** and **Bz6**-catalyst systems.

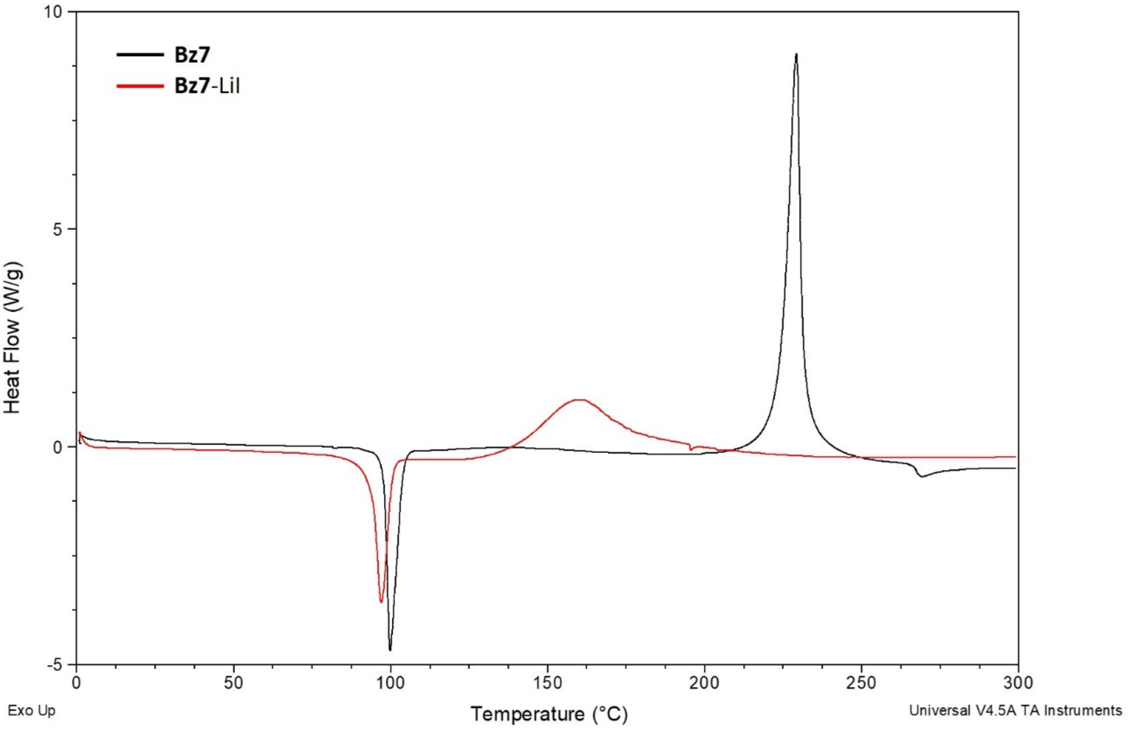

Fig. S18 DSC thermogram of neat **Bz7** and **Bz7**-catalyst systems.

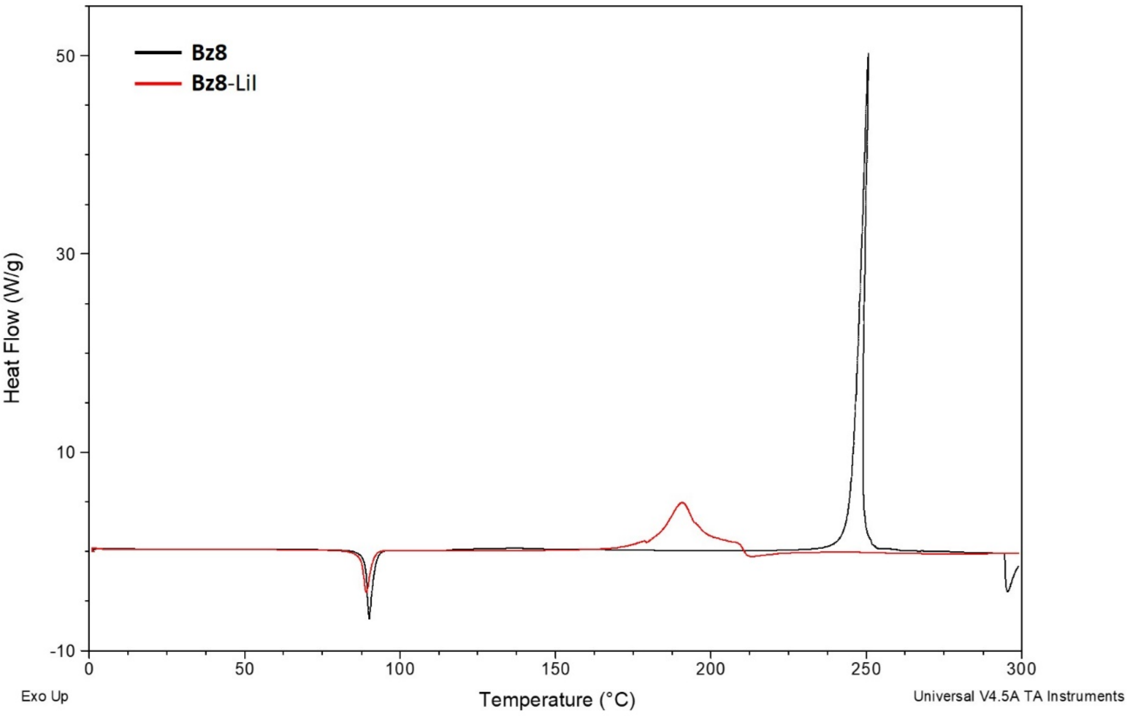

Fig. S19 DSC thermogram of neat **Bz8** and **Bz8**-catalyst systems.

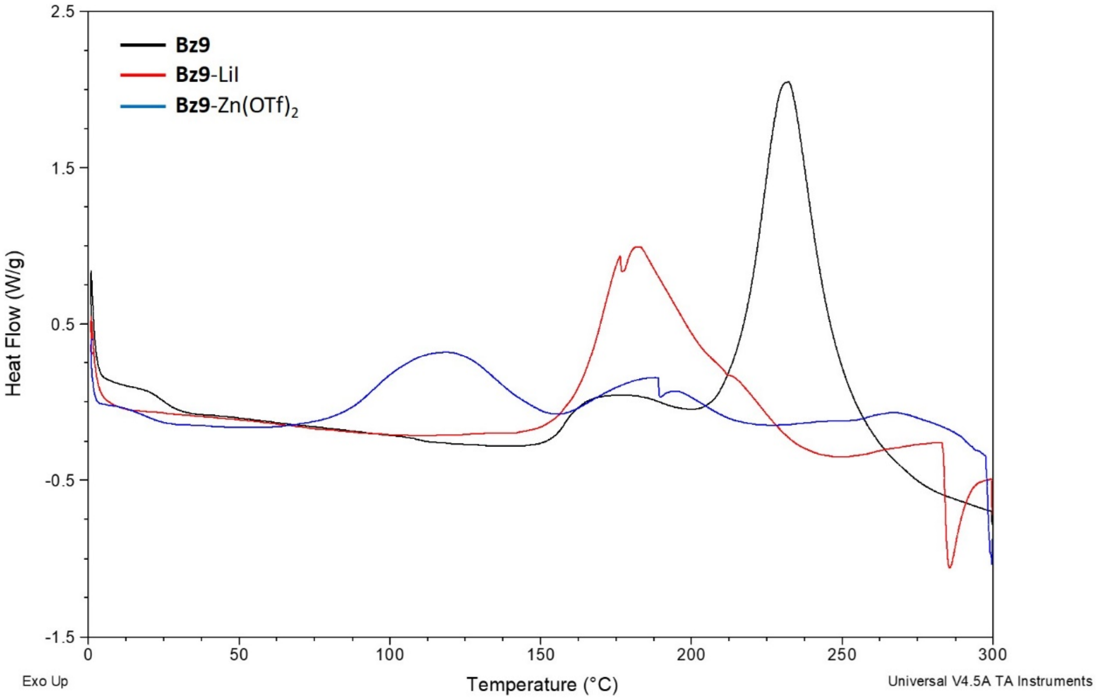

Fig. S20 DSC thermogram of neat **Bz9** and **Bz9**-catalyst systems.

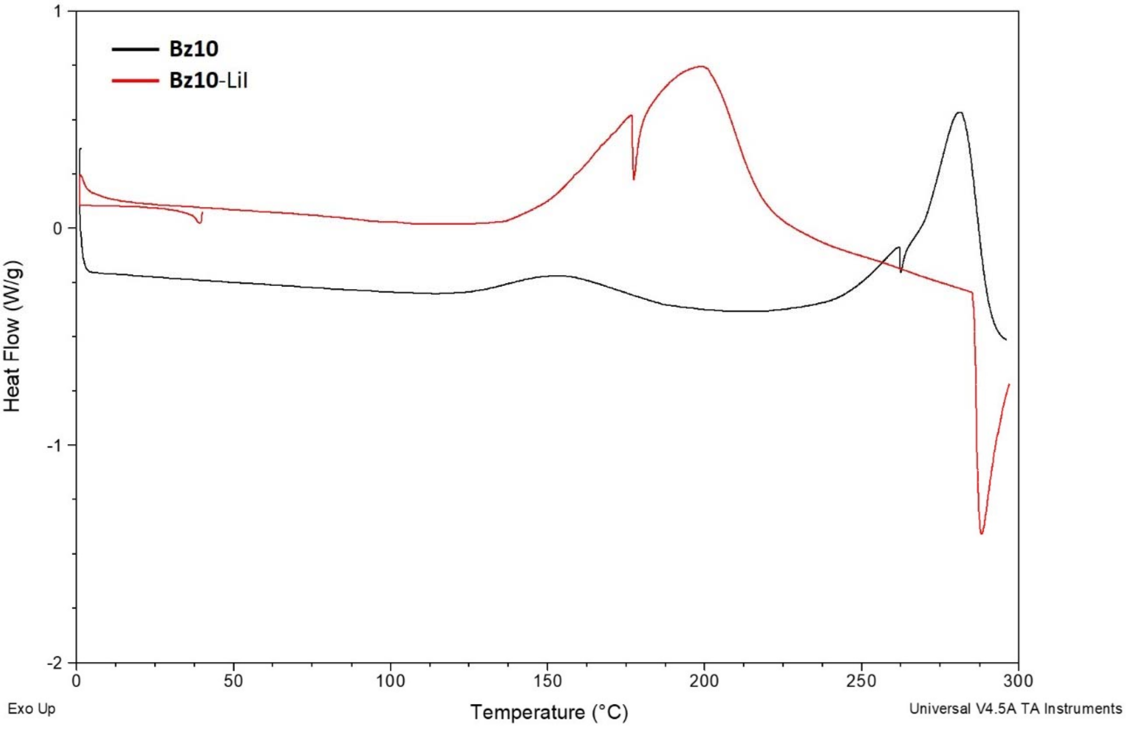

Fig. S21 DSC thermogram of neat **Bz10** and **Bz10**-catalyst systems.

4.4. Photothermal polymerization

General procedure: Each of the neat Bz monomers or monomer-catalyst systems (prepared as described in section 4.1 were placed either within a glass cuvette (50 x 0.8 x 0.4 mm) for solid samples (**Bz1**, **Bz2** and **Bz4-Bz9**, 0.2 – 0.3 g) (Fig. S22a) or within a glass vial (Ø = 1 cm) for liquid samples (**Bz3** and **Bz10**, 0.5 mL) (Fig. S22b). Then, they were irradiated with a pulsed green laser under ambient conditions for the required time (Fig. S22c).

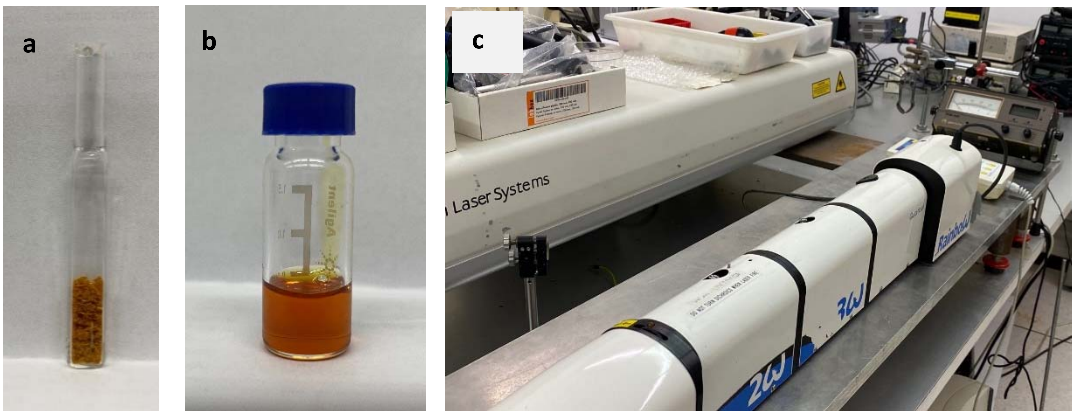

Fig. S22 (a) Solid and (b) liquid samples used in the photothermal polymerization experiments, which were mainly conducted employing (c) the 2nd harmonic of a ns-pulsed Nd:YAG laser as an irradiation source.

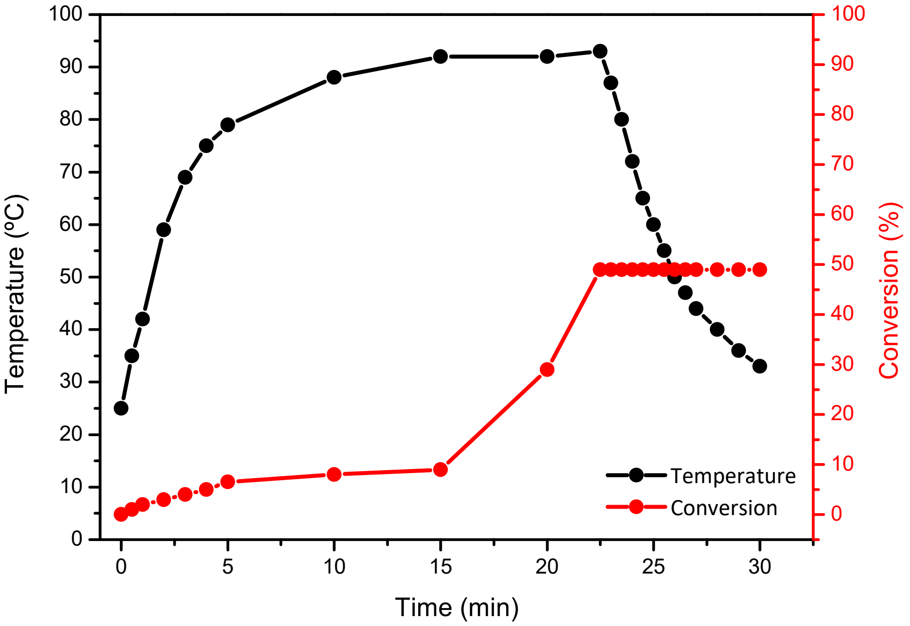

Fig. S23 Evolution of the reaction mixture temperature and monomer conversion during visible light irradiation of **Bz3**-LiI (c_{LiI} = 15 mol % relative to monomer concentration; λ_{exc} = 532 nm, power density = 1.1 W cm^{-2}). At t_{irr} = 22.5 min when ca. 50% of monomer conversion had been reached, irradiation was stopped, which resulted in a sudden termination of the polymerization process and a more gradual decrease of temperature.

Frontal polymerization experiments: To investigate the self-propagation capacity of the photothermal polymerization process, frontal polymerization experiments were carried out. In these experiments, only a small region of the Bz-catalyst samples was irradiated to induce photopolymerization, while the monomer conversion was investigated for the nonirradiated area (Fig. S24).

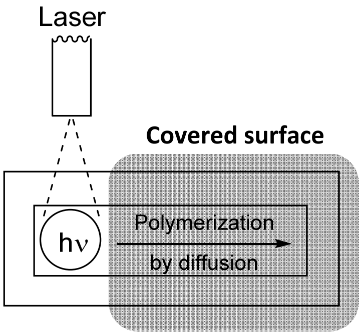

Fig. S24 Schematic representation of a frontal polymerization experiment. Pulsed laser irradiation of a specific area was conducted for 100 min (λ_{exc} = 532 nm, $\varnothing_{spot}$ = 1 cm, power = 1.1 W cm^{-2}).

4.5. Chemical stability of Bz3-catalyst systems

Benzoxazine **Bz3** was mixed with LiI (15 mol % relative to monomer concentration) and $Zn(OTf)_2$ (15 mol % relative to monomer content), respectively, in 2-3 mL of deuterated acetone. Both solutions were stirred for several days at room temperature. ^1H NMR analysis were performed every 24 h in order to check the intensity variation of benzoxazine peaks at δ ~ 5.4 and 4.6 ppm.

5. Analysis of polybenzoxazines

5.1. Determination of the phenoxy-phenolic structure ratio

The phenoxy-phenolic structure ratio of photothermally polymerized PBz-catalyst samples[e] and their annealed products was determined by a variation of the procedure developed in previous studies in our research group.7,8 The ^{1}H NMR signals located between δ ~ 4.0 – 6.0 ppm and 3.5 – 4.0 ppm were assigned to phenoxy-type CH_2 and phenolic-type CH_2 units, respectively. If *m* and *n* represent the signal integration of these phenoxy and phenolic CH_2 units, respectively, the phenoxy-to-phenolic ratio can be obtained as (in %): $[m/(m+n)]\cdot 100$ (Figs. S25-S28). Other typical signals found in the ^{1}H NMR spectra of polybenzoxazines are found at: (a) δ ~ 6.0 – 8.0 ppm, which arise from the aromatic protons of the polymers; (b) δ ~ 8.0 – 9.5 ppm, which are generally attributed to residual imine formation during the polymerization process.[9]

Thermal annealing of photothermally produced **PBz1-PBz4** was performed by heating up the corresponding polymers at 150 °C for 2 h. It must be noted that this resulted in the disappearance of most of the resonances in the δ ~ 4.0 – 6.0 ppm region, thus indicating thermal phenoxy-to-phenolic conversion of the polymer structure.

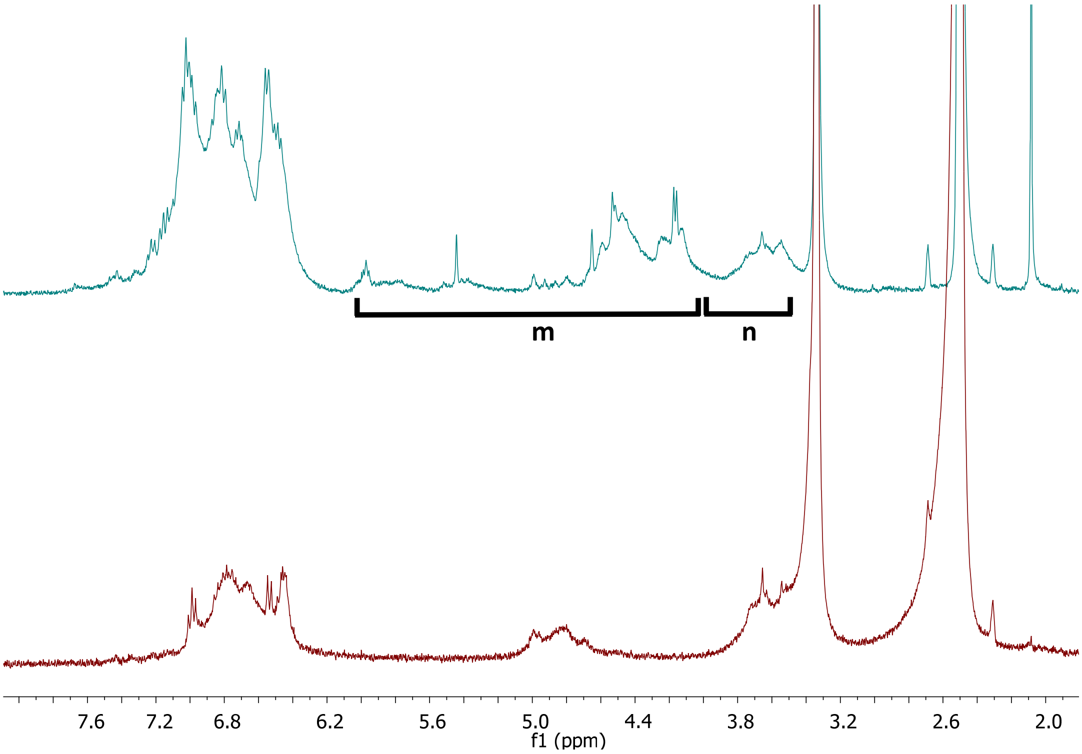

Fig. S25 ^{1}H NMR spectra (360 MHz, DMSO-d_6) of the PBz obtained by photothermal polymerization of **Bz1**-LiI (blue) and subsequent thermal annealing (red).

---

[e] Phenoxy-phenolic structure ratio of the photothermally polymerized **Bz9**-LiI system and its annealed product could not be measured due to their poor solubility in all solvents.

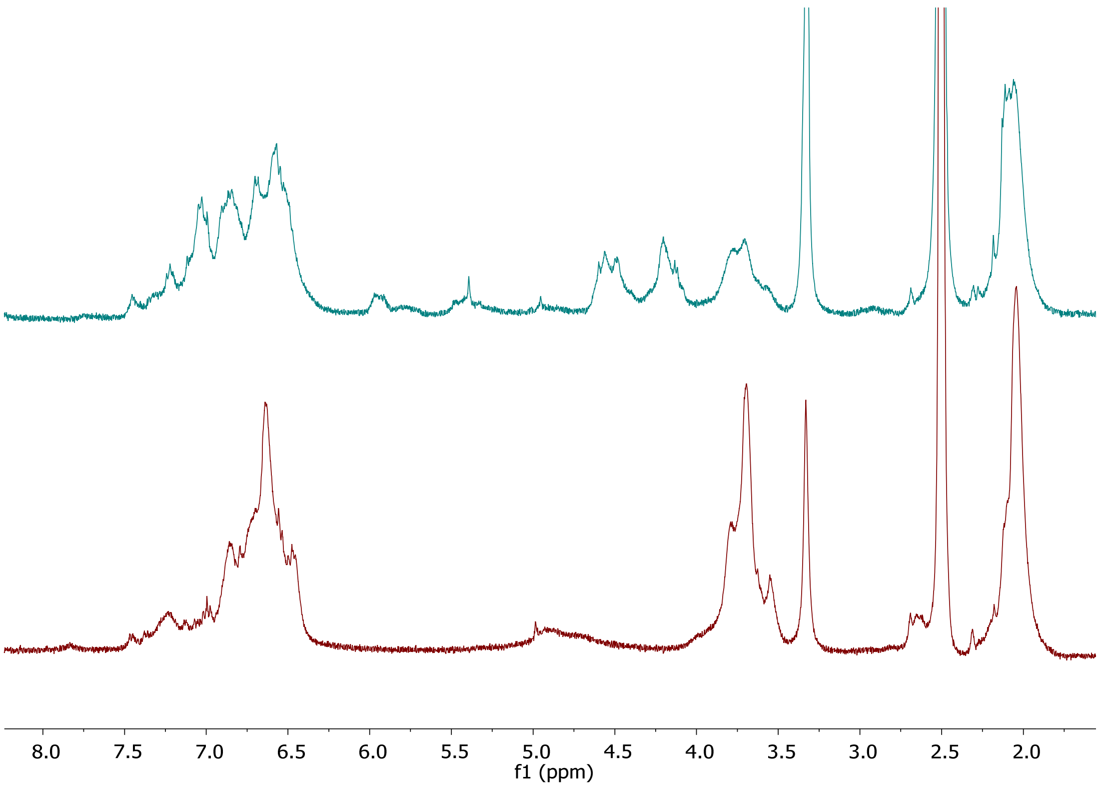

Fig. S26 ^{1}H NMR spectra (360 MHz, DMSO-d_6) of the PBz obtained by photothermal polymerization of **Bz2**-LiI (blue) and subsequent thermal annealing (red).

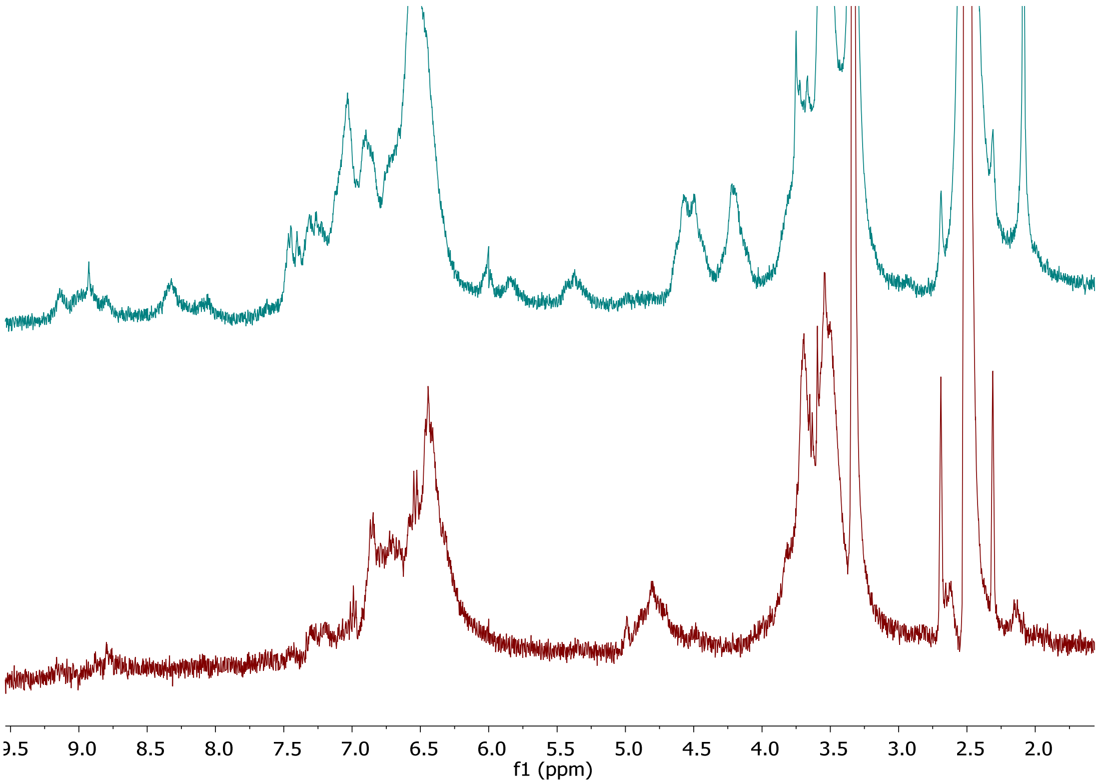

Fig. S27 ^{1}H NMR spectra (360 MHz, DMSO-d_6) of the PBz obtained by photothermal polymerization of **Bz3**-LiI (blue) and subsequent thermal annealing (red).

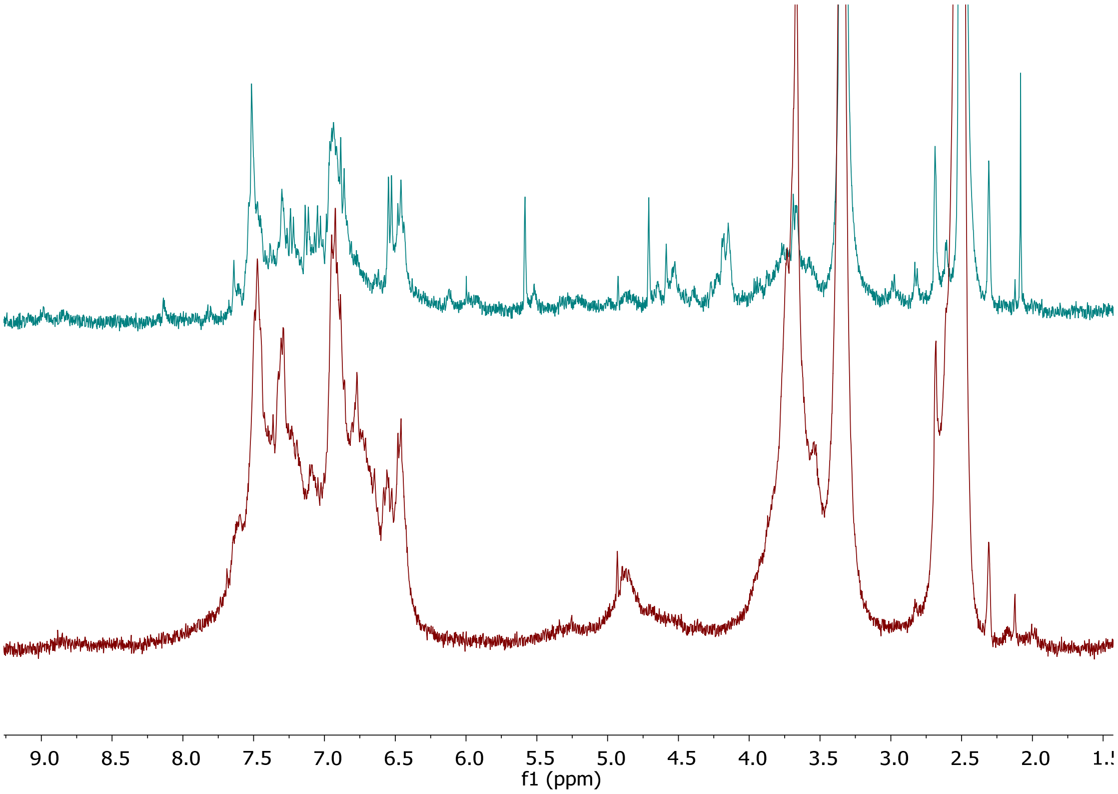

Fig. S28 ^{1}H NMR spectra (360 MHz, DMSO-d_6) of the PBz obtained by photothermal polymerization of **Bz4**-LiI (blue) and subsequent thermal annealing (red).

5.2. Determination of T_g

Transition glass temperatures of thermally-polymerized **PBz1-PBz4** and **PBz9** and photothermally-polymerized **PBz1-PBz4** and **PBz9** were measured by DSC analysis (Figs. S29-S33).

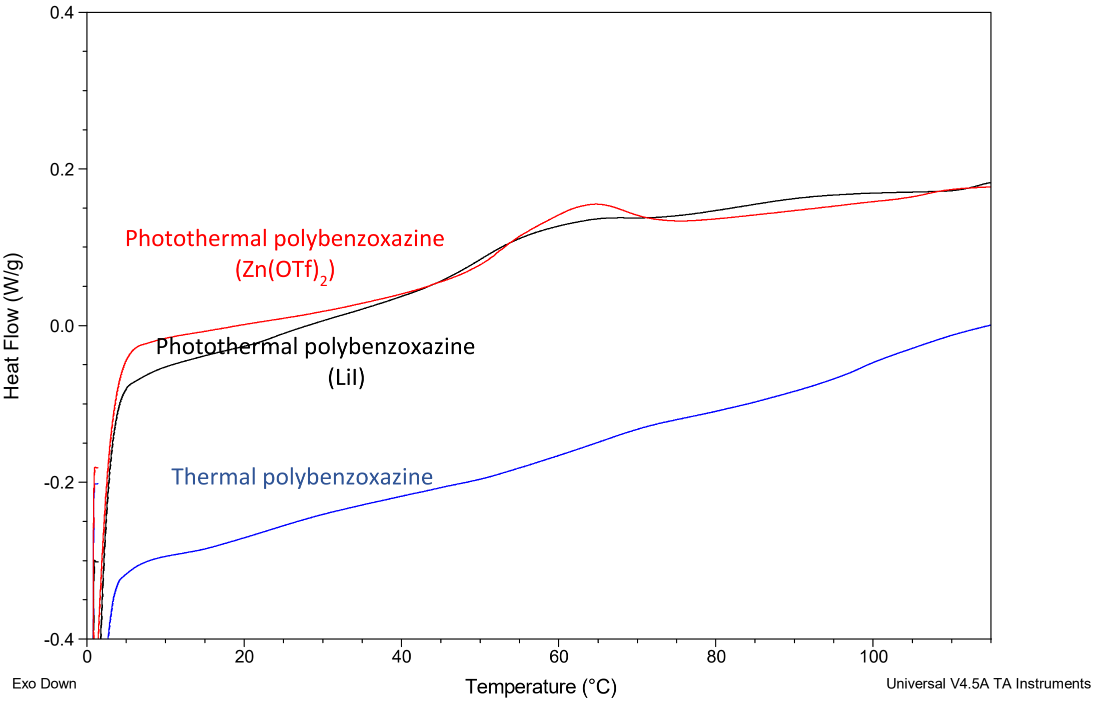

Fig. S29 DSC thermograms of the PBz materials obtained through the thermal (no catalyst) and photothermal polymerization of **Bz1**.

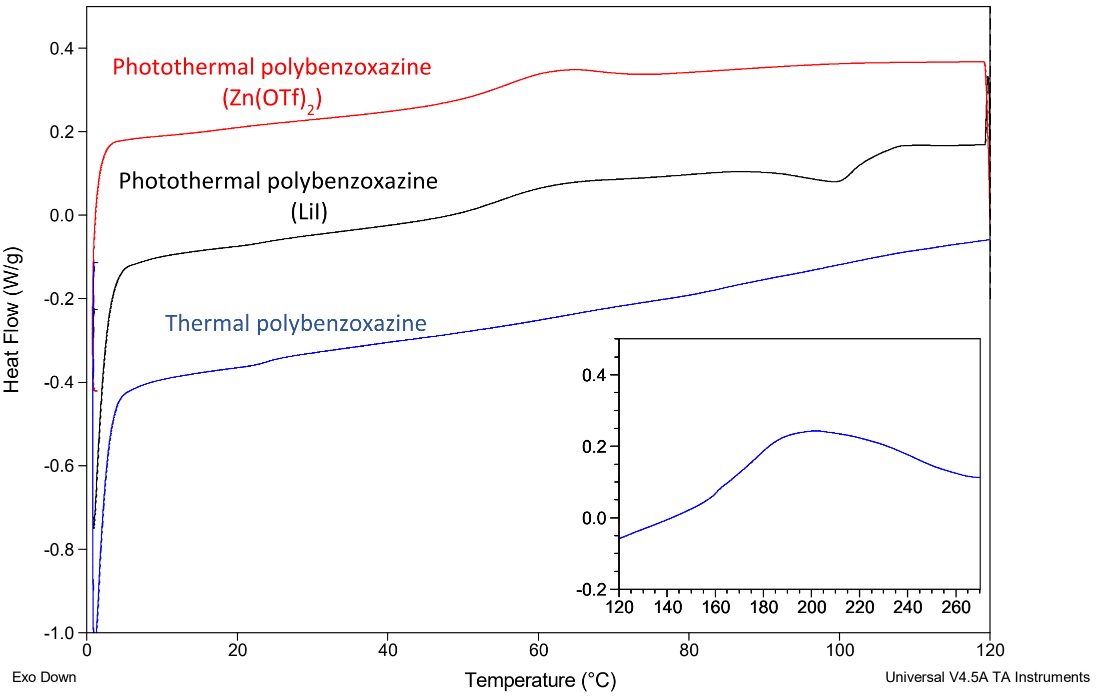

Fig. S30 DSC thermograms of the PBz materials obtained through the thermal (no catalyst) and photothermal polymerization of **Bz2**.

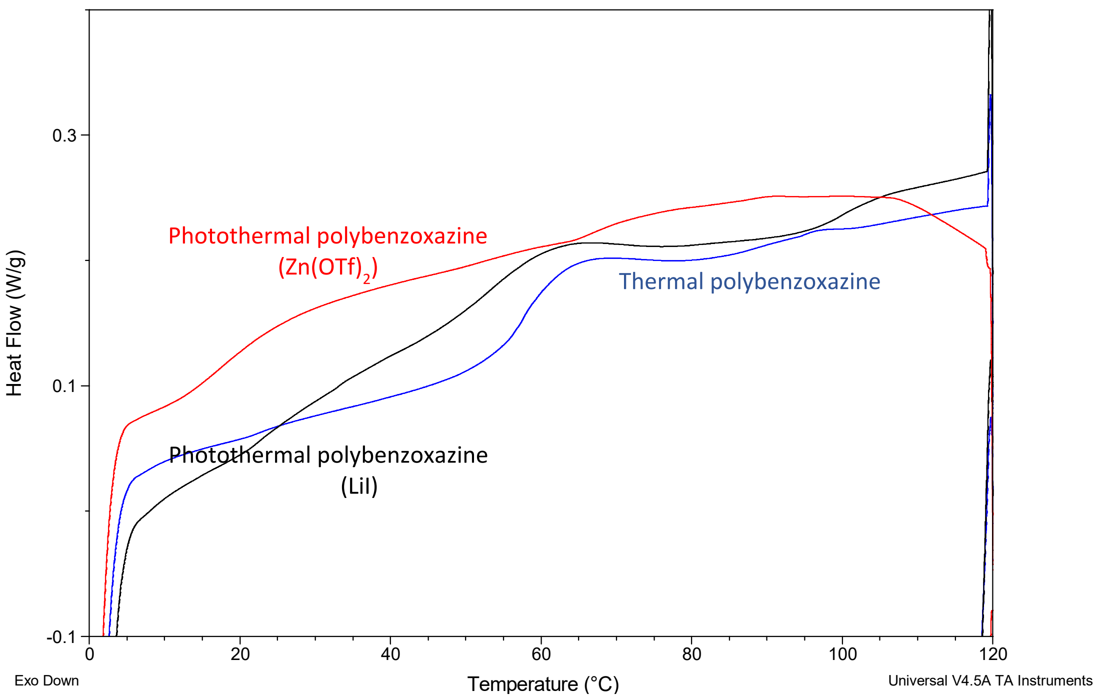

Fig. S31 DSC thermograms of the PBz materials obtained through the thermal (no catalyst) and photothermal polymerization of **Bz3.**

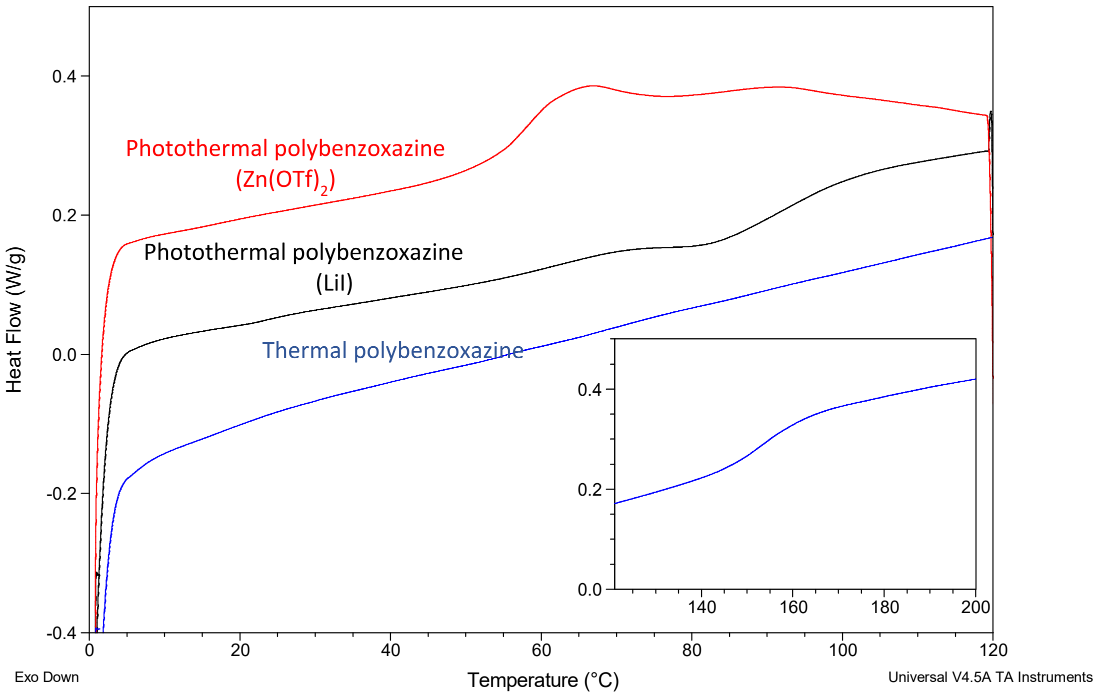

Fig. S32 DSC thermograms of the PBz materials obtained through the thermal (no catalyst) and photothermal polymerization of **Bz4**.

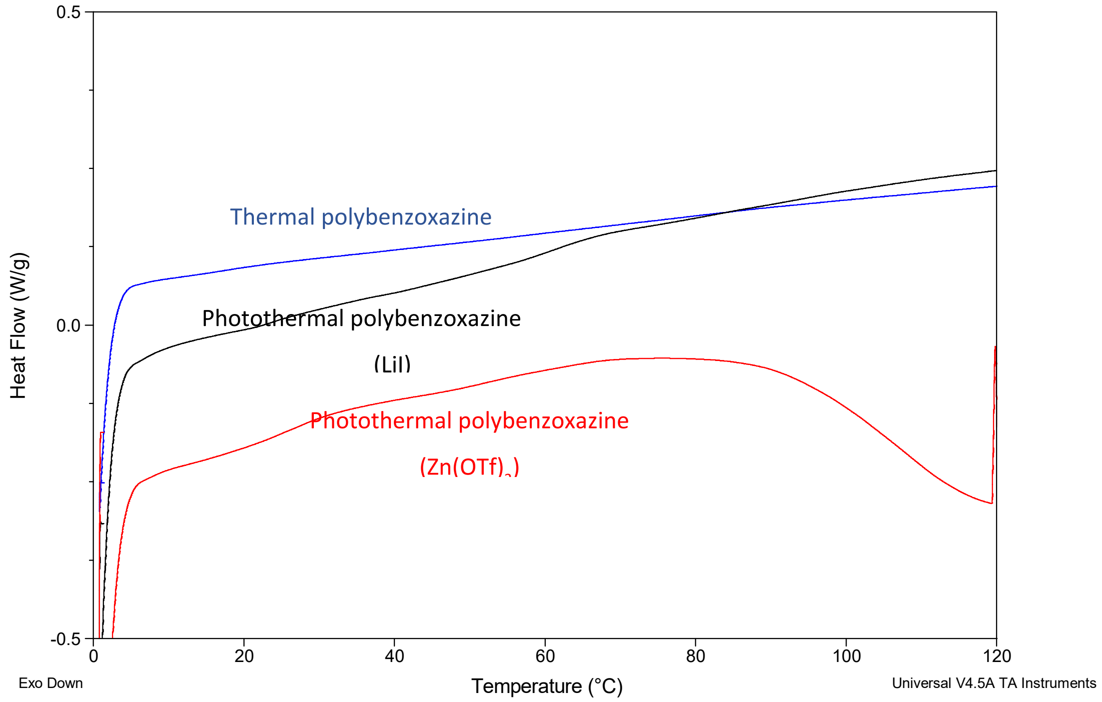

Fig. S33 DSC thermograms of the PBz materials obtained through the thermal (no catalyst) and photothermal polymerization of **Bz9**.

5.3. Determination of char yield and thermal decomposition

The char yields of thermally-polymerized **PBz1-PBz4** and **PBz9** and photothermally-polymerized **PBz1-PBz4** and **PBz9** were registered by thermogravimetric analysis (Figs. S34-S38). To assess the thermal stability of the polymers, we shown in Table S3 the temperatures for 5% and 10% weight loss determined from the TGA measurements.

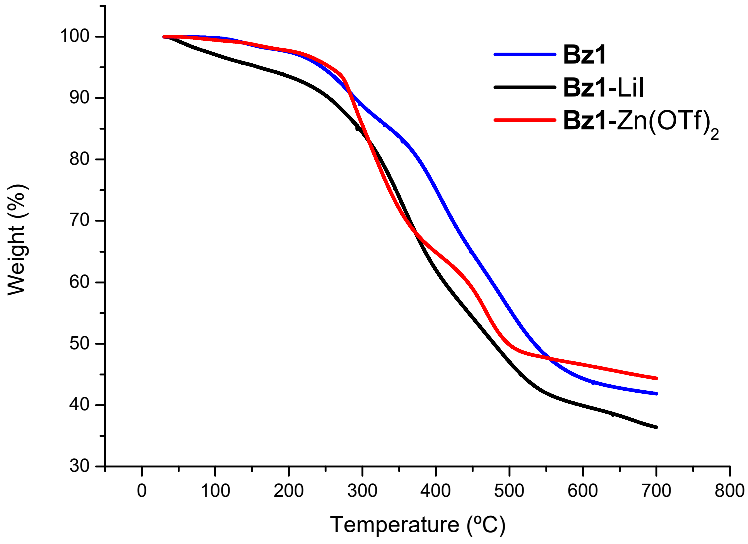

Fig. S34 TGA thermograms of the PBz materials obtained through the thermal (no catalyst) and photothermal polymerization of **Bz1**.

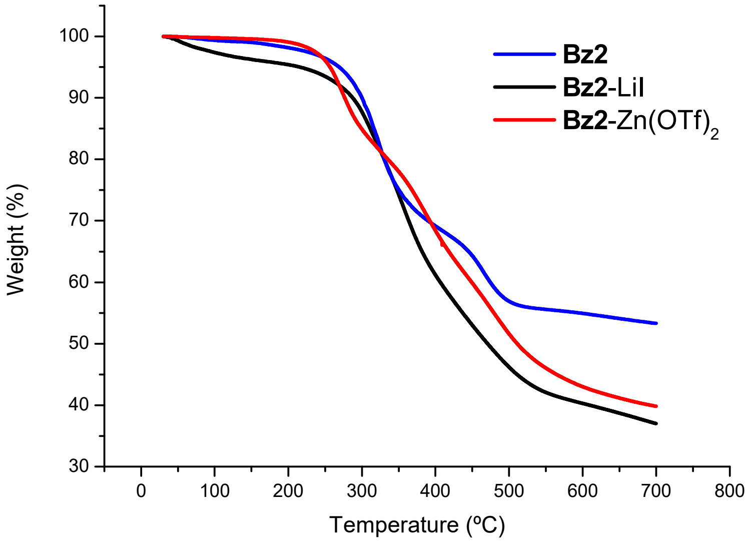

Fig. S35 TGA thermograms of the PBz materials obtained through the thermal (no catalyst) and photothermal polymerization of **Bz2.**

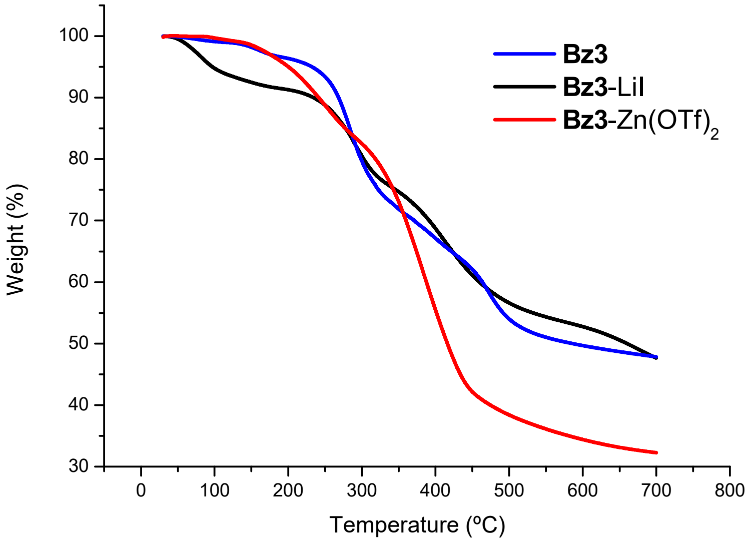

Fig. S36 TGA thermograms of the PBz materials obtained through the thermal (no catalyst) and photothermal polymerization of **Bz3**.

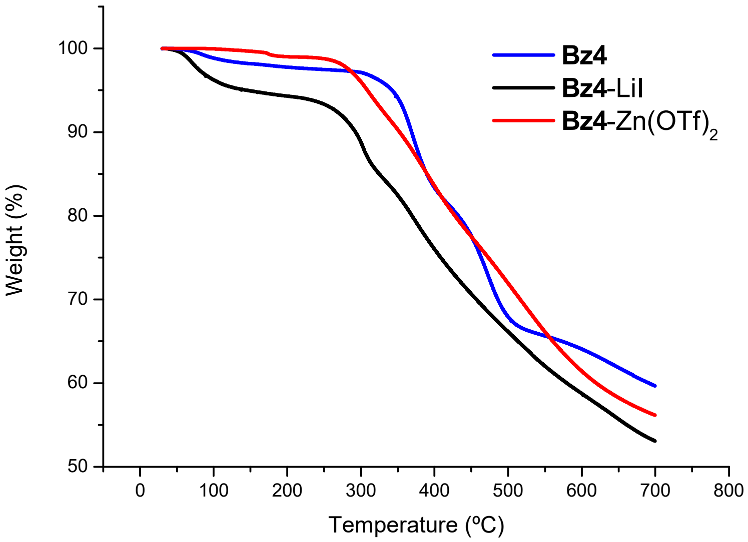

Fig. S37 TGA thermograms of the PBz materials obtained through the thermal (no catalyst) and photothermal polymerization of **Bz4**.

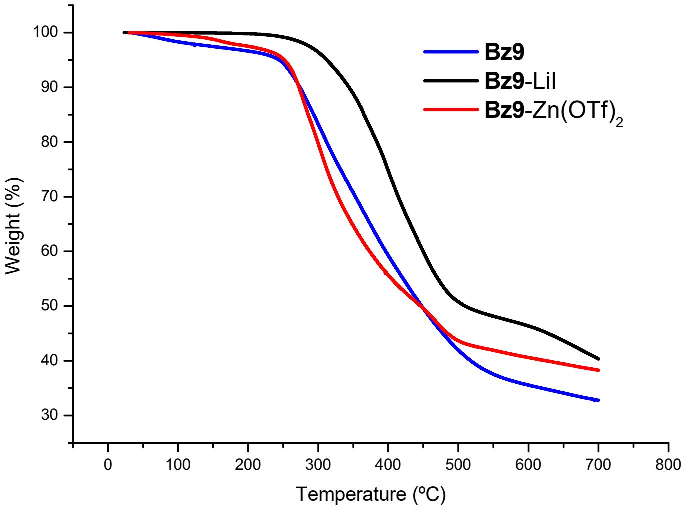

Fig. S38 TGA thermograms of the PBz materials obtained through the thermal (no catalyst) and photothermal polymerization of **Bz9**.

Table S4. $T_{5\%}$ and $T_{10\%}$ of neat thermal **PBz1-PBz4** and **PBz9** and their photothermal PBz-catalyst systems.

Bz	Catalyst	$T_{5\%}$ (°C)	$T_{10\%}$ (°C)
Bz1	-	246	290
	LiI	159	255
	$Zn(OTf)_2$	256	286
Bz2	-	257	277
	LiI	216	288
	$Zn(OTf)_2$	269	300
Bz3	-	232	269
	LiI	97	234
	$Zn(OTf)_2$	200	241
Bz4	-	342	369
	LiI	145	293
	$Zn(OTf)_2$	309	353
Bz9	-	312	344
	LiI	244	274
	$Zn(OTf)_2$	252	273

5.4. Determination of gel content

The gel content of selected photothermally- and thermally-prepared polymers was determined as previoulsy reported by us.[10] About 0.7 g of the polymer material of interest were subjected to a 24 h Soxhlet extraction using acetone as a solvent. This led to dissolution of linear polymer chains, leaving behind the insoluble cross-linked 3D network. Therefore, comparison of the final insoluble material left in the cellulose cartridge used in the extraction (m_{gel}) with the initial polymer mass (m_0) allowed us the calculation of the gel content using equation (3):

$$Gel\ content\ (\%) = \frac{m_{gel}}{m_0} \cdot 100 \qquad (3)$$

5.5. Purification of polymer-catalyst samples

To explore the purification of polymer-catalyst samples, we selected the polymer material obtained from the photopolymerization of the **Bz3**-$Zn(OTf)_2$ system ($c_{Zn(OTf)2}$ = 15 mol %) as a benchmark case. About 0.5 g of this material were suspended within 5 mL of cold acetone and the resulting mixture was stirred for 4 h in an ice bath. After this time, most of the initial polymer had been dissolved, which was separated from the remaining solid by filtration. After solvent evaporation of the filtrate, the dissolved polymer was analyzed by ^{1}H NMR and ^{19}F NMR in DMSO-d_6 and the obtained spectra were compared with those registered before purification. In the case of ^{19}F NMR, a controlled quantity of trifluoroacetic acid (10 µL) was added as an internal standard to quantify the decrease in the integral of the signal corresponding to the triflate anions after purification.

6. Photolithography experiments

Photolithography experiments were performed with a NEJE Master 2/2s laser-engraving machine equipped with a focusable 405 nm cw laser (33 W cm^{-2}) and the NEJE v5.6 software (Fig. S39). Samples were prepared by depositing a **Bz3**/**Bz9**-Zn(OTf)$_2$ formulation onto a glass substrate (9:1 **Bz3**:**Bz9** ratio, c_{catalyst} = 15 mol % relative to the total monomer content), which was then subjected to photolithography experiments. To remove the excess of unreacted monomer-catalyst system, the samples were gently rinsed with an organic solvent (e.g., ethyl acetate).

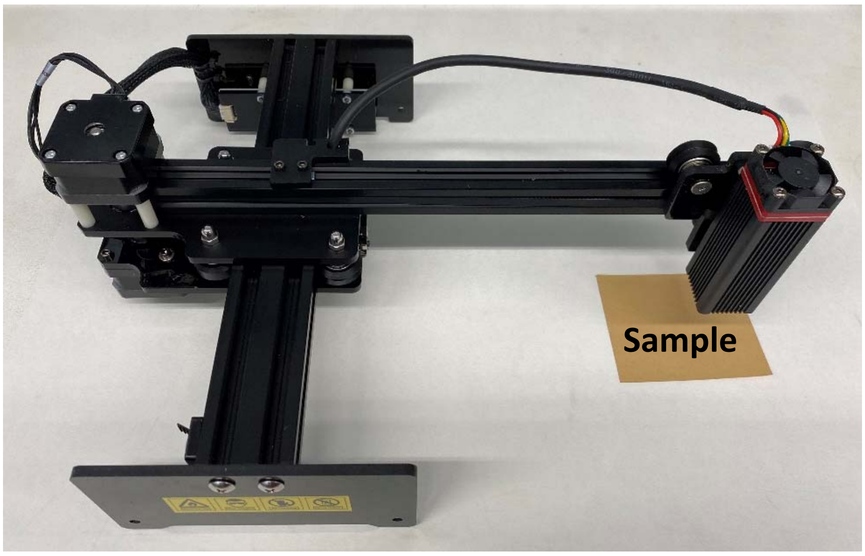

Fig. S39 Image of the laser-engraving machine used for the photolithography experiments.

7. NMR spectra

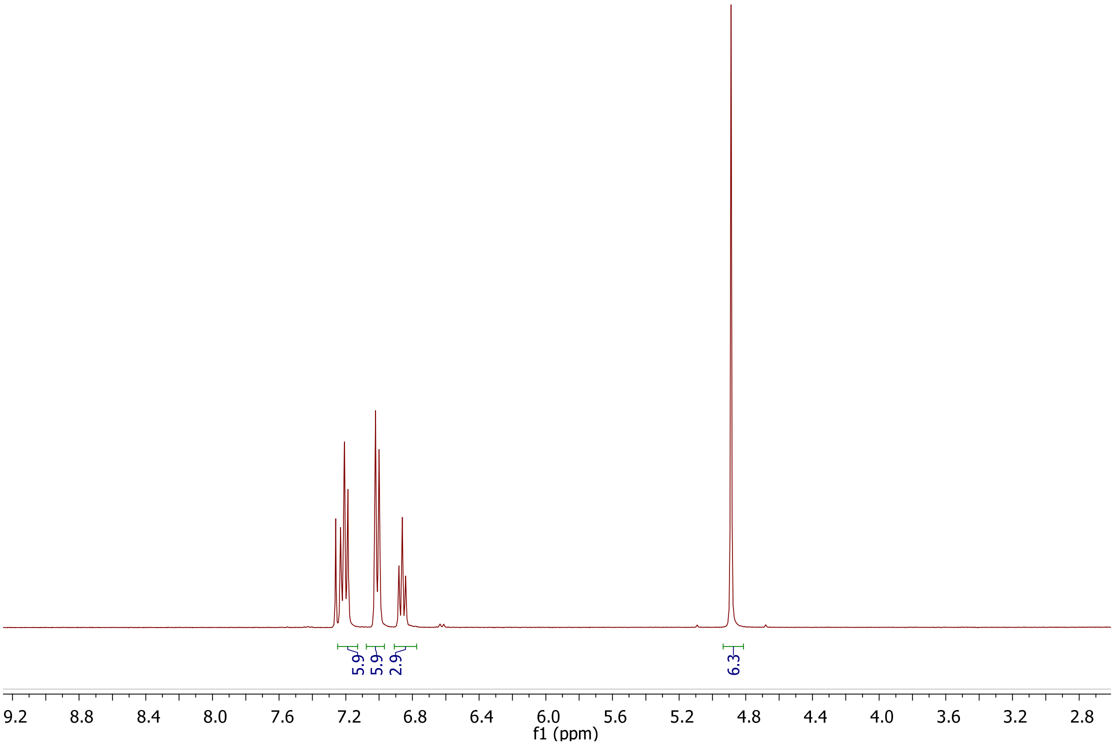

Fig. S40 ^{1}H NMR spectrum (360 MHz, $CDCl_3$) of 1,3,5-triphenyltriazine (**3**).

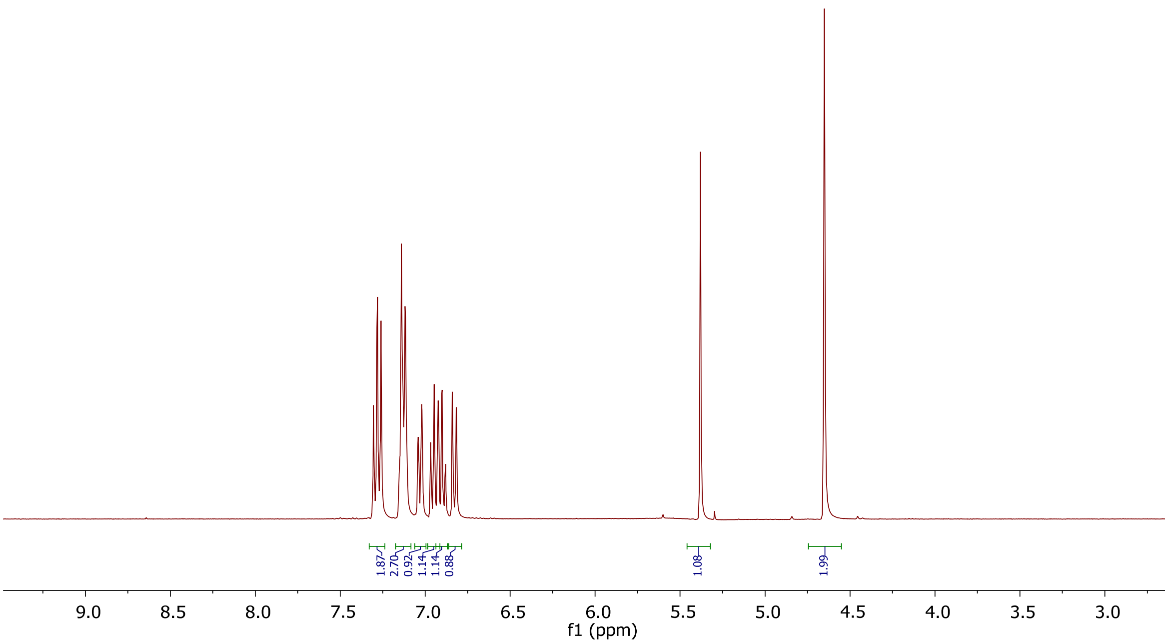

Fig. S41 ^{1}H NMR spectrum (360 MHz, $CDCl_3$) of **Bz1**.

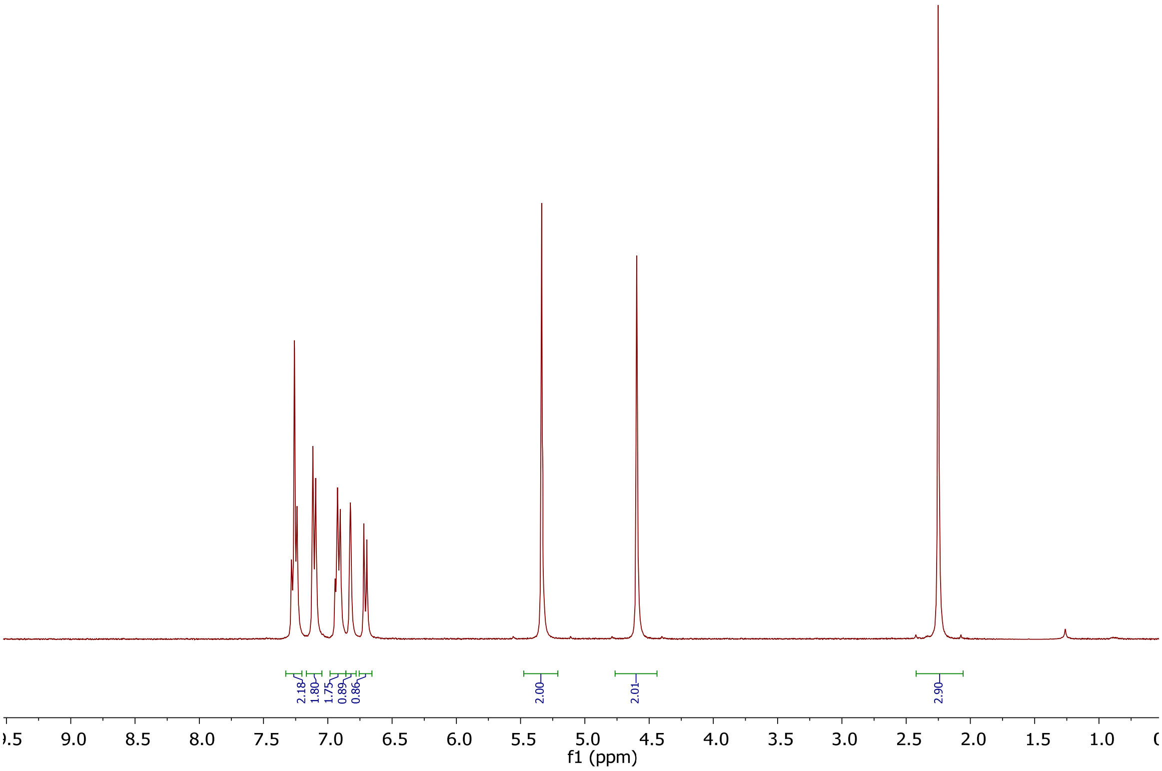

Fig. S42 ^{1}H NMR spectrum (360 MHz, $CDCl_3$) of **Bz2**.

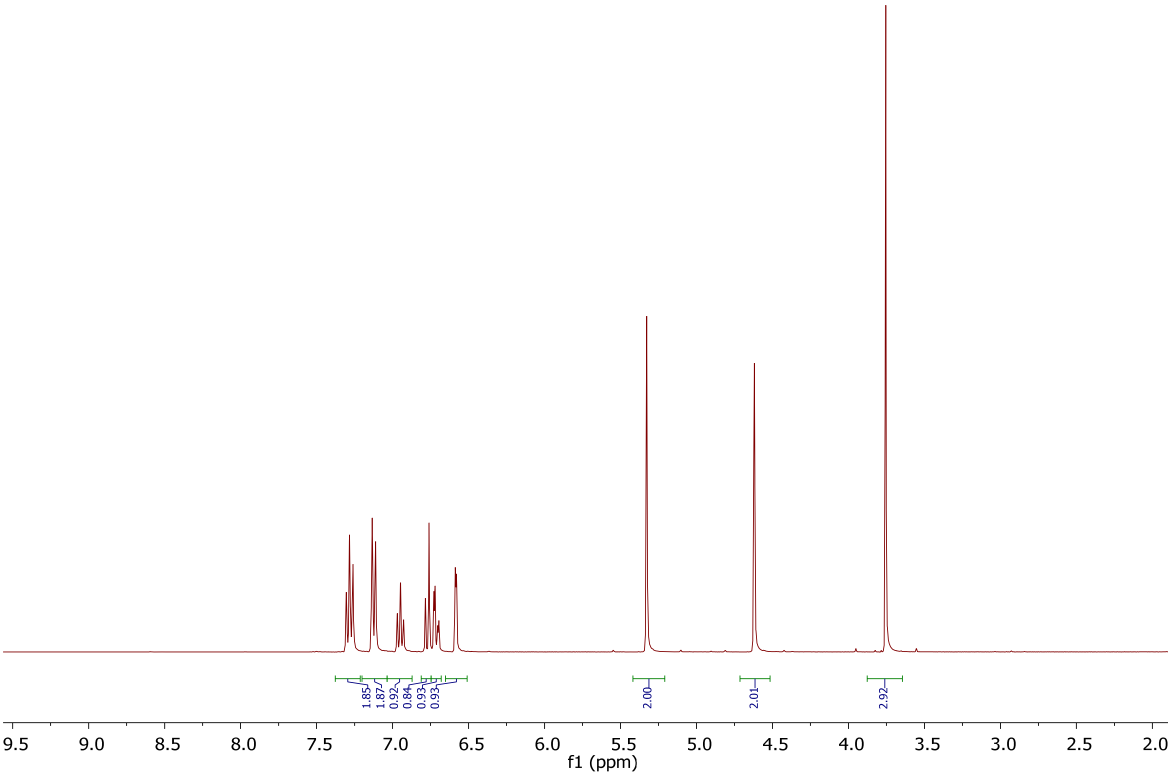

Fig. S43 ^{1}H NMR spectrum (360 MHz, CDCl$_3$) of **Bz3**.

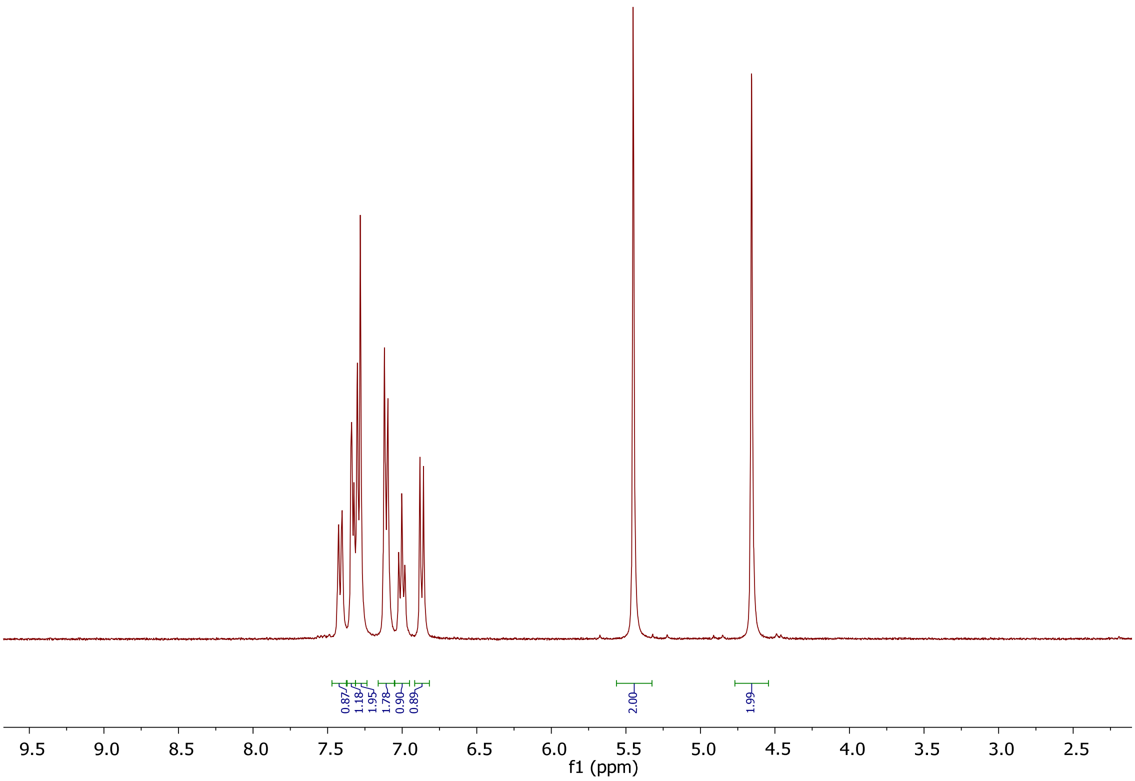

Fig. S44 ^{1}H NMR spectrum (360 MHz, CDCl$_3$) of **Bz4**.

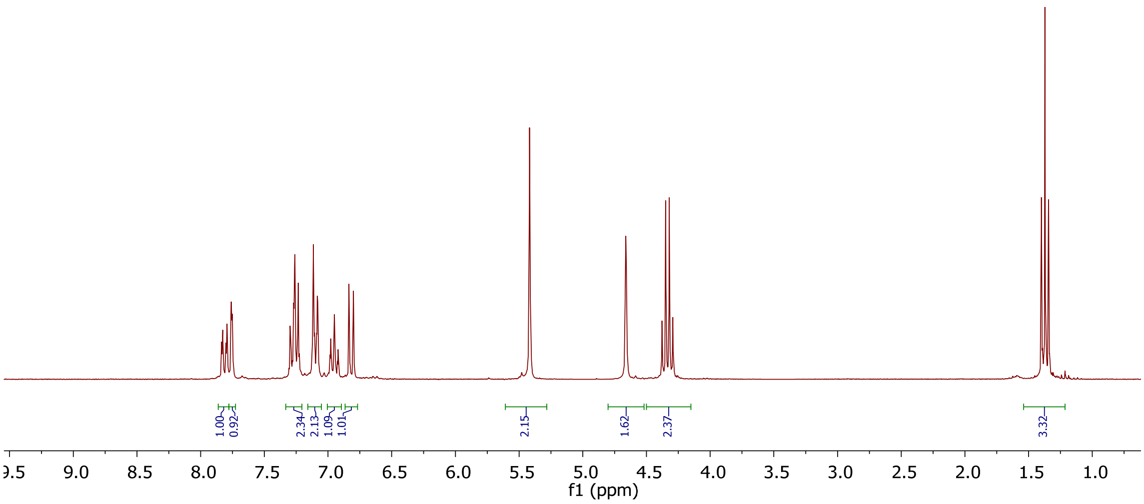

Fig. S45 ^{1}H NMR spectrum (360 MHz, $CDCl_3$) of **Bz5**.

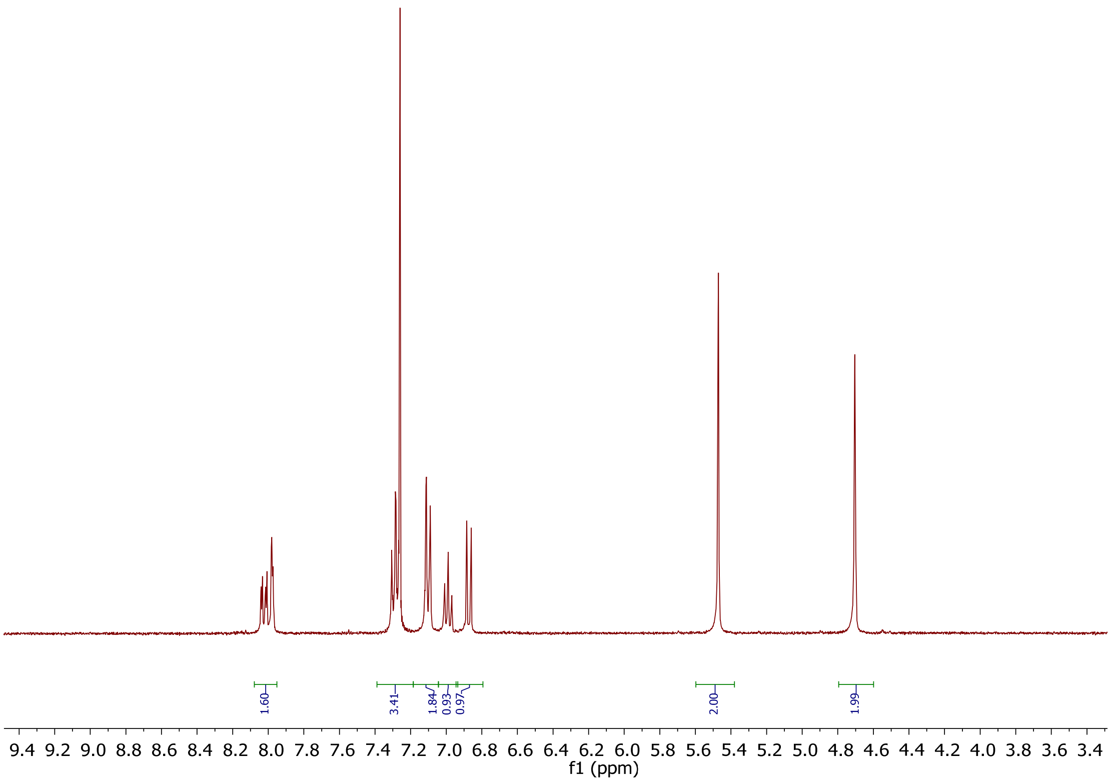

Fig. S46 ^{1}H NMR spectrum (360 MHz, $CDCl_3$) of **Bz6**.

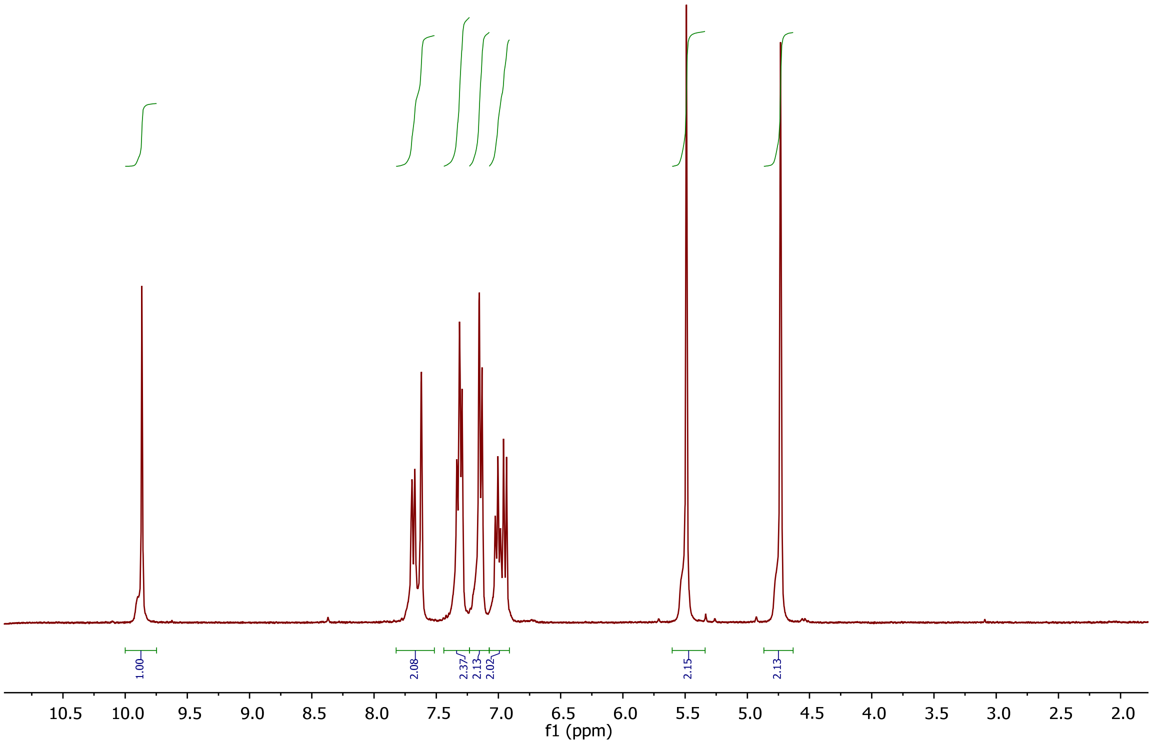

Fig. S47 ^{1}H NMR spectrum (250 MHz, $CDCl_3$) of **Bz7**.

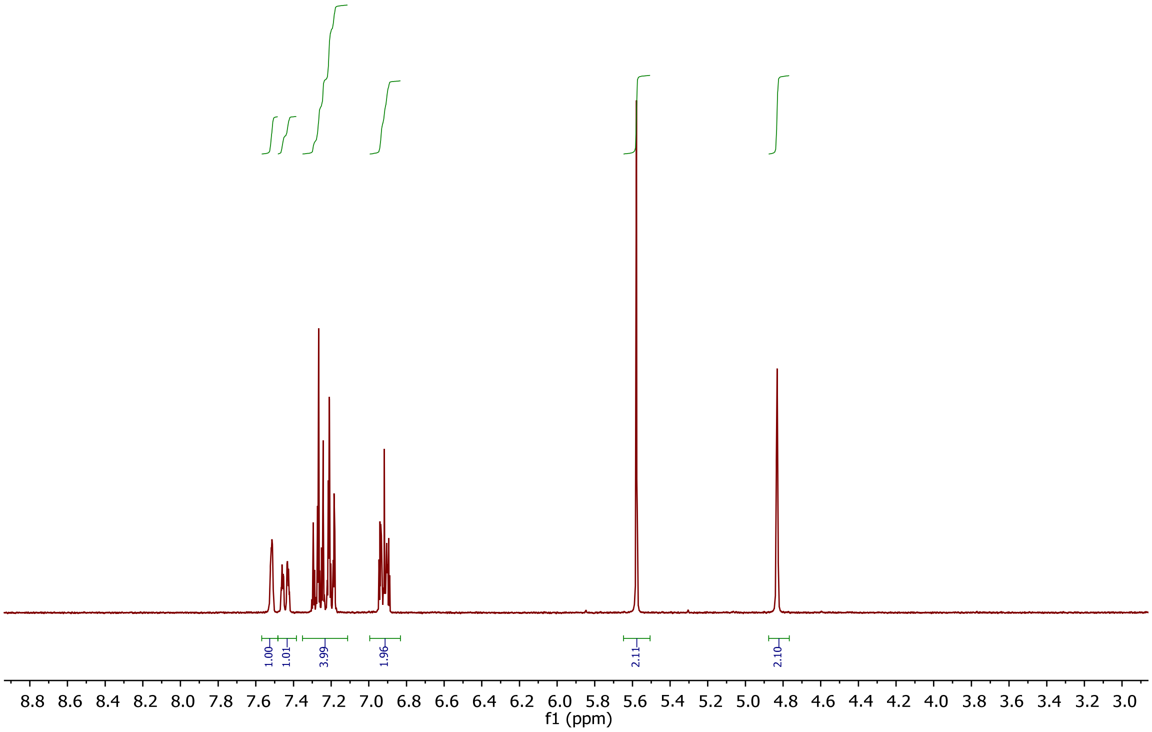

Fig. S48 ^{1}H NMR spectrum (300 MHz, $(CD_3)_2CO$) of **Bz8**.

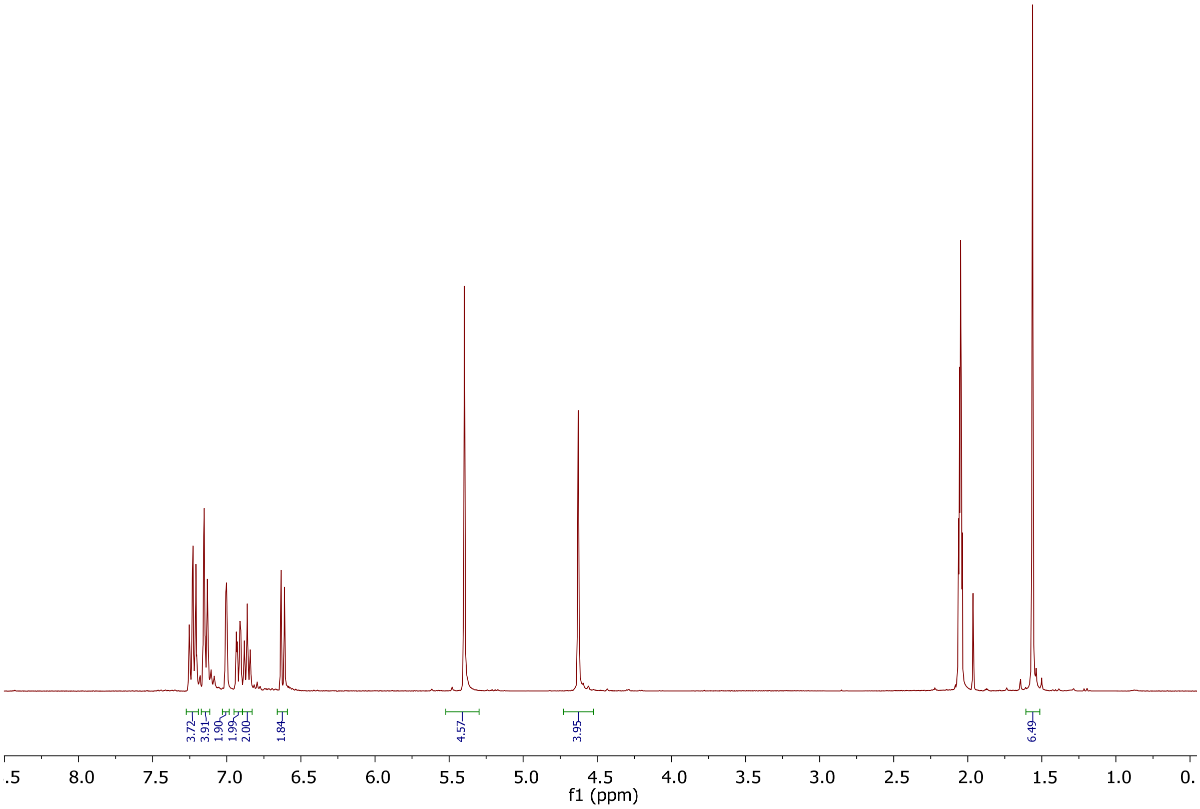

Fig. S49 ^{1}H NMR spectrum (360 MHz, $CDCl_3$) of **Bz9**.

8. References

[1] R. Andreu, J. A. Reina and J. C. Ronda, *J. Polym. Sci. A: Polym. Chem.*, 2008, **46**, 3353-3366.

[2] M. A. Espinosa, V. Cádiz and M. Galia, *J. Appl. Polym. Sci.*, 2003, **90**, 470-481.

[3] J. Salabert, R. M. Sebastián and J. Marquet. *Macromolecules*, 2018, **51**, 3672-3679.

[4] A. Martos, R. M. Sebastián and J. Marquet. *Eur. Polym. J.* 2018, **108**, 20-27.

[5] H. M. Ma, Y. Liu, Y. X. Liu, J. J. Qiu and C. Liu, *RSC Adv.*, 2015, **5**, 102441-102447.

[6] P. Chutayothin and H. Ishida, *Macromolecules*, 2010, **43**, 4562-4572.

[7] C. Liu, D. Shen, R. M. Sebastián, J. Marquet and R. Schönfeld, *Polymer*, 2013, **54**, 2873−2878.

[8] C. Liu, D. Shen, R. M. Sebastián, J. Marquet and R. Schönfeld. *Macromolecules*, 2011, **44**, 4616−4622.

[9] P. Chutayothin and H. Ishida, *Macromolecules*, 2010, **43**, 4562-4572.

[10] A. Martos, M. Soto, H. Schäfer, K. Koschek, J. Marquet and R. M. Sebastián, *Polymers*, 2020, **12**, 254.